universität wien

MASTERARBEIT / MASTER'S THESIS

Titel der Masterarbeit / Title of the Master's Thesis

„Combinatory effects of the mycotoxins alternariol and deoxynivalenol and the microbial metabolite urolithin A on the integrity of the intestinal epithelial barrier in Caco-2 cells“

verfasst von / submitted by

Carina Seidl, B.Sc.

angestrebter akademischer Grad / in partial fulfilment of the requirements for the degree of

Master of Science (MSc)

Wien, 2023 / Vienna 2023

Studienkennzahl lt. Studienblatt / degree programme code as it appears on the student record sheet:	UA 066 659
Studienrichtung lt. Studienblatt / degree programme as it appears on the student record sheet:	Masterstudium Lebensmittelchemie
Betreut von / Supervisor:	Univ. Prof. Dr. Doris Marko

Acknowledgements

Zunächst möchte ich mich bei Prof. Dr. Doris Marko für die Möglichkeit bedanken, mein Masterpraktikum am Institut für Lebensmittelchemie und -toxikologie zu absolvieren und die Welt der Forschung kennenzulernen. Des Weiteren danke ich Prof. Dr. Giorgia Del Favero, die mich herzlich in ihr Team aufgenommen hat und stets ihre Leidenschaft für der Forschung versprüht. Außerdem möchte ich ein großes Dankeschön an die gesamte Arbeitsgruppe für die angenehme Atmosphäre und kollegiale Unterstützung richten. Ganz besonders dankbar bin ich meiner Betreuerin Julia Gröstlinger, PhD, die mir sowohl fachlich als auch menschlich und persönlich zur Seite stand, selbst über ihre eigene Zeit an der Universität Wien hinaus. Vielen herzlichen Dank, liebe Julia!

Und zu guter Letzt natürlich all meinen Liebsten, meinen Eltern, meinem Umfeld, meinen Freund*innen, von HCL bis zu den Crannies, die mit mir Geduld hatten, mich in Zeiten des Zweifels bekräftigt und stets ihre bedingungslose Hilfsbereitschaft betont haben. Für immer Danke, dass ihr meine Stütze wart und seid. Merci!

Abstract

The infestation with moulds and consequent contamination with mycotoxins is a problem that affects about 25 % of the global crop production each year. Not only do these contaminants cause loss of production, many of them also harbour extensive risks for human and animal health. This work investigated the impact of two frequently detected mycotoxins, deoxynivalenol (DON) and alternariol (AOH), on the intestinal barrier. The health status of the intestine together with its intertwined inflammatory state strongly correlates with our nutrition but also our microbiome. That is why urolithin A (UroA), a microbial metabolite formed from polyphenolic ellagitannins, was included in addition. Amongst the examined parameters were the enzyme activity of a group of CYP isoforms as well as protein expression of CYP1A1 and the tight junction protein ZO-1. These are factors contributing to the barrier function on a molecular level and were investigated in an *in vitro* model of differentiated Caco-2 cells mimicking the human intestinal epithelium.

The results revealed that UroA as well as AOH, at a concentration of 25 µM each, significantly increased enzyme activity in a 7-ethoxy-resorufin-*O*-deethylase (EROD) assay after 48 h of incubation. When combined with 2.5 µM DON, enzyme activity remained at control level. Simultaneously, exposure to DON and AOH alone led to a decrease in the protein expression of CYP1A1 and ZO-1. Different scenarios of binary treatment with AOH, DON and UroA did not affect CYP1A1 protein levels. However, all binary combinations yielded elevated protein expressions of ZO-1 compared to the control and at least one of the respective substances alone. Further, it could be confirmed that AOH and UroA act as regulators of the aryl hydrocarbon receptor (AhR). The effect of AOH and UroA on EROD enzyme activity was shown to be AhR-dependent through the application of the AhR antagonist CH223191. For AOH, AhR-dependency was also determined for the expression of the assessed proteins.

The results of this study demonstrate that food contaminants such as mycotoxins pointedly attack the intestinal barrier. Beyond that, possible approaches to counteract such impairments are discussed. These might include targeted modification of involved signalling pathways or the implementation of natural, bioactive substances into the human diet.

Contents

1 Introduction

The topic of food safety became more and more prominent over the past decades and keeps on gaining attention. With new global challenges, the factors compromising the safety of food and feed keep changing and growing and new aspects appear (Crudo et al. 2019). With advancing climate change, geographical conditions shift causing increasing impairment for established agricultural systems. As explained by van der Fels-Klerx et al. (2016), predictive models expect alterations in temperature and precipitation, for instance, to become more extreme than observed so far. On the one hand, this can have a hazardous impact on food safety by affecting harvest yield. On the other hand, changes in environmental conditions indirectly affect agricultural production via impacts on the crops' susceptibility to pests and plant diseases as well as shifts in fungal populations and their patterns of mycotoxin production. Despite operating analytical measures and continuous efforts to reduce and eliminate contaminated foodstuff before it reaches the customer, it cannot be prevented completely. Therefore, the gastrointestinal tract (GIT) and especially the intestinal epithelium present the "next" line of defence for the human or animal body after the consumption of food contaminants (Springler et al. 2016).

In humans, the route of foodstuffs upon ingestion leads through the oesophagus to the stomach, where the degradation is enhanced by the acidic milieu and greater presence of digestive enzymes (Farré et al. 2020). From there, the chyme enters the intestine where the main absorption processes of nutrients occur before reaching the colon and ensuing excretion. However, compounds and their metabolites that already reached the circulatory system are potentially reintroduced to the gut lumen via the biliary duct (Koppel et al. 2017). Subsequently, they might be reabsorbed in the small intestine, entering the enterohepatic circulation or they continue on to the colon and are excreted with the faeces (Koppel et al. 2017).

1.1 The Intestinal Epithelial Barrier

The intestine as a main site of absorption plays a crucial role in distinguishing between beneficial, nutritious compounds and harmful, exogenous molecules. This highly complex regulation relies on the interplay of various factors. The "intestinal barrier" comprises of

the gut microbiome which is the entity of microorganisms colonizing the gut, the mucus layer covering the intestinal wall, the epithelium and the immunological network resident in the underlying lamina propria (Gao et al. 2020). The epithelium is a single-cell layer composed of different epithelial cell types and presents an actual physical barrier (Lamas et al. 2018; Mayorgas et al. 2021). Beside mucus secreting goblet cells, antimicrobial peptides (AMPs) producing Paneth cells and hormone-releasing enteroendocrine cells, enterocytes constitute the greatest proportion of the cell layer and are responsible for the absorption of molecules from the lumen along with possible transport to the basolateral side (Gao et al. 2020; Farré et al. 2020).

The integrity of this layer of epithelial cells is supported by protein structures in the intercellular space sealing the gaps between neighbouring cells (Odenwald and Turner 2017; McLaughlin et al. 2004). In these gaps, being broader in the more basolateral regions than at the apical end (Farré et al. 2020), three distinguishable junctional sites occur, composing the apical junctional complex. From basolateral to apical, these are: desmosomes, zonula adherens (adherens junctions) and zonula occludens (tight junctions, TJs) (Odenwald and Turner 2017). While desmosomes and adherens junctions contribute mainly to the cells' adhesive capacities, TJs play an important role in regulating the paracellular transport routes (Odenwald and Turner 2017).

The tight junction complex poses the main determinant of the specificity in permeability between adjacent cells (Lee 2015b). Distinct selectivity in terms of charge and size of the molecules enabled to pass the intercellular space leads to two divergent paracellular pathways, the "pore" and the "leak" pathway (Odenwald and Turner 2017; Le Shen et al. 2011). While the pore pathway provides transport with high capacity as well as size- and charge-selectivity, the leak pathway poses a route of low capacity and lower selectivity (Le Shen et al. 2011). Upon impairment of the intestinal epithelium, for example due to disease-induced damage, an alternative third pathway, the so called "unrestricted" pathway, was previously described as well (Odenwald and Turner 2017). This pathway shows a non-regulated selectivity in terms of charge or size with a high capacity on top, thereby enhancing the risk of passage of bigger, exogenous molecules or even whole bacteria.

The TJ complex is composed of various protein families fulfilling various functions. Based on localisation of different tight junction proteins (TJP), it can be distinguished between transmembrane and scaffolding proteins (Odenwald and Turner 2017). Proteins belonging to the family of claudins (Cldn) are classified as transmembrane proteins. Their domains reaching the extracellular side were observed to build pores with adjacent cells determining the ion selectivity of the paracellular pathway (Le Shen et al. 2011; McLaughlin et al. 2004). Amongst the scaffolding proteins, members of the zonula occludens (ZO) protein family are interacting with transmembrane TJPs as well as the cells' cytoskeletal actin (Lee 2015b).

1.2 Inflammation

Intestinal inflammation can have a myriad of causes, many of which are prone to interfering with one another. Exogenous compounds or alterations in the composition of the microbiota residing in the GIT are just a glimpse of possible factors causing an imbalance of the intestinal homeostasis (Farré et al. 2020). Disruption of the intestinal barrier can trigger as well as reinforce existing inflammation in the mucosal environment (Ivanov et al. 2010). This can happen via various ways, all leading to increased immunomodulation. Besides disturbance of the immune response via physical damage to the cellular layer itself, leakages facilitate the translocation of luminal microbes, which might also include exogenous and possibly pathogenic microorganisms, to deeper mucosal layers (Amoroso et al. 2020). Some pathogens release disruptive compounds aiming at the epithelial barrier like pore-forming toxins or bacterial lipopolysaccharide (LPS) (Ivanov et al. 2010). In some cases, endogenous immune cells also contribute to an increased permeability of the epithelial barrier upon their activation to enable a more direct access to the site of invasion (Ivanov et al. 2010; Farré et al. 2020). However, all these ways lead to a common consequence which is an enhanced activation of the mucosal immune system. A central part of this immune response is the production and secretion of pro-inflammatory cytokines, such as tumor necrosis factor-α (TNF-α), interferon-γ (IFN-γ) or interleukin-1β (IL-1β), additionally exaggerating the initial inflammation (Amoroso et al. 2020; Ivanov et al. 2010). An impaired epithelial barrier is

most often associated with intestinal inflammation and *vice versa*, be it as an initiator or a result of the inflammatory condition.

Upon persisting inflammation, diseases or symptoms related to a disturbed immune response might manifest. Prominent cases of gastrointestinal disorders of inflammatory origin are chronic intestinal bowel diseases (IBD), essentially Crohn's disease (CD) and ulcerative colitis (UC), provoking symptoms like diarrhoea, abdominal pain and weight loss (Schoultz and Keita 2019). These complex conditions are suggested to be a result of dysregulated immune responses, especially in genetically susceptible patients (Amoroso et al. 2020). Apart from IBD, an impaired intestinal barrier and concomitant increased permeability is also found in other pathogenic conditions such as food allergies, coeliac disease, irritable bowel syndrome and various infections with enteric pathogens (Ivanov et al. 2010; Farré et al. 2020).

A large number of signalling pathways is involved in the response to and regulation of inflammatory processes. One of them is the mitogen-activated protein kinases (MAPKs) signalling cascade which subdivides into three major classes: p44/42 ERK, p38 and JNK (Springler et al. 2016). The p44/42 ERK subfamily is especially interesting in relation to intestinal barrier function as it is involved in the regulation of proliferation, morphology and differentiation of intestinal epithelial cells (IECs) and further in the structure of the intercellular tight junctions (Springler et al. 2016; Pinton et al. 2012). Upon activation in the cytosolic compartment, MAPKs are able to translocate to the nucleus where they can activate further target molecules like transcription factors controlling various cell functions (González-Sarrías et al. 2009b). MAPK activation is associated with an increase in the expression of pro-inflammatory cytokines as well as enzyme activity (van de Walle et al. 2008). Moreover, MAPKs regulate other pathways involved in inflammatory responses like the nuclear factor-κB (NF-κB) pathway. Activation of the NF-κB transcription factor is induced by external stimuli such as the inflammatory cytokine IL-1β while causing an increased expression of inflammatory mediators as well (van de Walle et al. 2008; González-Sarrías et al. 2010b). Elevated activity of this transcription factor has been described as a key feature of IBD (Schreiber et al. 1998).

Many compounds that could be identified as being responsible for anti- or pro-inflammatory effects, exerted for instance by heterogenous food matrices or the sum

of metabolites originating from mould infestation, were found to interact with different steps of pathways involved in the inflammatory response. Findings of that kind not only contribute to elucidating certain compounds' modes of action but also reveal possible approaches for therapeutic treatments of disease patterns rooting in such processes.

1.3 The Aryl Hydrocarbon Receptor (AhR)

The gastrointestinal environment is one of the key sites of our immune response, not least because it is eminently confronted with exogenous compounds. A crucial player in the regulation of intestinal homeostasis is the aryl hydrocarbon receptor (AhR), a transcription factor particularly abundant in different intestinal cell types (Stockinger et al. 2021). Initially, it was primarily associated with metabolism of xenobiotic, rather detrimental molecules like polycyclic aromatic hydrocarbons (PAHs) or the AhR agonist 2,3,7,8-tetrachlorodibenzo-p-dioxin (TCDD) (Muku et al. 2018; Lamas et al. 2018). This view was broadened however, by identifying a multitude of natural compounds whose activation of the AhR resulted in protective effects on mucosal immunity or upregulation of TJPs (Stockinger et al. 2021). Additionally, experiments inducing AhR-deficiency revealed increased susceptibility to inflammatory conditions. Nonetheless, consistent AhR-activation also dysregulates the elaborate signalling pathway (Stockinger et al. 2021).

The AhR is activated by ligand-binding which triggers its translocation from the cytosolic to the nuclear compartment where the ligand-AhR-complex dimerizes with the AhR nuclear translocator (ARNT) protein (Lamas et al. 2018). This structure then binds to respective genomic recognition sites directing the transcription of target genes encoding, amongst others, for phase I metabolism enzymes like the cytochrome P450 (CYP) enzyme family with several isoforms such as CYP1A1, CYP1A2 and CYP1B1 (Lamas et al. 2018). As shortly touched on before, implications of AhR activation are ambiguous and strongly context-dependent. For the intracellular regulation of this complex signalling pathway, three negative feedback mechanisms have been described so far: I) degradation of activating ligands by CYP enzymes, II) hindering the formation of the AhR-ARNT-complex by competitive binding of the AhR repressor (AhRR) to ARNT, III) proteasomal degradation of the AhR protein itself (Lamas et al. 2018; Stockinger et al. 2021).

Amongst the before mentioned natural ligands it can further be distinguished between a plant-based or an endogenous origin, the latter often synthesized through gut-microbial metabolization of dietary compounds which therefore act as “pro-ligands” (Stockinger et al. 2021). Mycotoxins, for instance, are taken in through the consumption of contaminated foodstuffs. In this regard, AOH has been identified as a potent activator of the AhR and hence potential ligand (Schreck et al. 2012). Further findings suggested the involvement of the AhR in the induction of CYP1A1 by AOH in murine hepatocytes. This hypothesis was supported by Pahlke et al. (2016), finding a significant reduction of CYP induction caused by AOH in AhR-suppressed oesophageal cells as well as by a study of Hohenbichler et al. (2020) in which AOH dose-dependently enhanced CYP1 enzyme activity in breast cancer cells suggesting the activation of the AhR signalling pathway. In non-cancerous HCEC-1CT human colon epithelial cells, AOH was observed to trigger the nuclear translocation of the AhR (Groestlinger et al. 2022b). On the contrary, other compounds that show AhR-activating properties, for example metabolites of the essential amino acid tryptophane, are formed endogenously (Krautkramer et al. 2021). However – as stressed by Stockinger et al. (2021) – not all molecules that are able to activate the AhR pathway might effectively be direct ligands of the receptor; alternatively, indirect coherences can also result in induction of respective reporter signalling. Another example for an endogenous, microbially generated AhR-inducing compound is urolithin A (UroA), which has been determined as a direct ligand of the AhR by Muku et al. (2018) and will be elucidated in more detail hereinafter (see chapter 1.4.1).

1.4 The Microbiome and its Food-Derived Metabolites

As mentioned above, inherent microbes are an important part of the human intestinal environment, constituting the gut microbiome. Although the microbiome comprises various microbial species including fungi, archaea, yeasts and viruses, the bacterial component within is the best enlightened so far (Clarke et al. 2019). The human GIT is inhabited by an estimated number of 10^{13} bacteria with the highest density in the large intestine (Clarke et al. 2019; Koppel et al. 2017). As a symbiotic partner, the gut microbiome in its entirety provides a multitude of functions vital for the hosts physiology in a supporting but also complementing manner. These include immunomodulatory

effects, colonization resistance and concomitant pathogen defence, metabolization and breakdown of dietary compounds as well as the synthesis of nutrients, e.g. vitamins (Koppel et al. 2017; Mayorgas et al. 2021). In addition, animal studies with germ-free mice revealed an influence on the expression or activity of metabolic host enzymes as the absence of microorganisms leads to up- or downregulation therefrom (Clarke et al. 2019). Having said this, it is not the microorganism itself that provokes these effects, but primarily molecules originating from it, hence microbial metabolites (Clarke et al. 2019; Krautkramer et al. 2021). According to Mayorgas et al. (2021), "microbial metabolites" describe any compound that is either synthesized *de novo* or modified by the microbiome. Bacterial metabolites can be divided into three groups: metabolites that are I) formed by bacteria from dietary constituents, II) generated through modification of host-derived molecules, III) synthesized *de novo* by the bacteria themselves (Mayorgas et al. 2021). Prominent examples of the last group are B vitamins, for instance folic acid (B9) (Krautkramer et al. 2021). Although it is also synthesized by the human body, the endogenous amount would be insufficient for optimal health and so the gut microbiota represents an important source of essential vitamins (Krautkramer et al. 2021). The gut microbiome can also extent the hosts metabolic capabilities as for instance by degrading bigger, diet-derived molecules like fibres or polyphenols for which enzymes of a human host are deficient (Krautkramer et al. 2021). Microbial fermentation of fibres like polysaccharides often yield short chain fatty acids (SCFAs), especially acetate, butyrate and propionate (Krautkramer et al. 2021). SCFAs play a regulatory role in multiple physiological host functions many of which support the maintenance of the intestinal barrier (Krautkramer et al. 2021). Another example are metabolic products of the amino acid tryptophane like indoles which are known to activate the AhR, posing one possibility of how the microbiome can interfere with and influence its hosts physiology (Krautkramer et al. 2021).

1.4.1 Urolithin A

Urolithin A (UroA) is a metabolite formed by certain species of the human gut microbiome from ellagitannins (ETs) and ellagic acid (EA) (Tomás-Barberán et al. 2017). EA and its precursor ETs are polyphenolic molecules present in several plants incorporated in an

average human diet like certain berries or nuts (Luca et al. 2020). Formation of UroA from EA takes place in multiple steps accomplished by various bacterial strains. Exemplarily, *Gordonibacter urolithinfaciens* is reported to degrade EA to the first urolithin intermediate (urolithin M5) while *Bifidobacterium pseudocatenulatum* INIA P815 was only recently discovered to actually form UroA (Aichinger 2021a; Gaya et al. 2018; Selma et al. 2014). In connection with consecutively detected UroA, the consumption of polyphenol-rich foods especially pomegranate, berries and walnuts plays a prevailing role (Espín et al. 2013). Polyphenols are well known for their antioxidant as well as other health beneficial properties like anti-inflammatory, anti-diabetic or cardioprotective effects (Luca et al. 2020). However, their bioavailability is very low, so it is hypothesized that their metabolites are responsible for their health effects to a great extent. This is also suggested for urolithins as they exert similar biological activity whilst showing higher bioavailability and prevalence in plasma and colon epithelial tissue compared to EA and ETs (Luca et al. 2020).

The group of urolithins comprises several derivatives, differing in their degree of hydroxylation. The first degradation product of EA is urolithin M5 with five hydroxy groups (Luca et al. 2020). Following this, multiple dehydroxylation reactions occur, generating several intermediates, eventually reaching UroA (OH groups at C3 and C8) or isourolithin A (isoUroA; OH groups at C3 and C9) and urolithin B (UroB; OH group at C3) (Furlanetto et al. 2012). The individual steps of the microbial metabolization of EA to UroA/UroB are depicted in Figure 1, taken from Espín et al. (2013). With a declining number of hydroxy groups, the molecules become more lipophilic, a state facilitating and enhancing their absorption. As the human microbiome is as unique as one's fingerprint, not everyone harbours urolithin-producing strains. Therefore, it can be distinguished between three different metabolic phenotypes, so called, "metabotypes" (0, A, B) (Tomás-Barberán et al. 2017). Metabotype A produces UroA, metabotype B generates UroA but also isoUroA and UroB while metabotype 0 does not form any of the stated metabolites. Additionally, a study by Tomás-Barberán et al. (2014) showed that some participants of the metabotype 0 could be converted to type A or B after high-dose supplementation of EA over longer periods. Others remained metabotype 0 despite supplementation, the so called "non-responders". Also, Cortés-Martín et al. (2018) observed an age-dependency

in the distribution of the different metabotypes showing an evident shift from type B to type A while type 0 appears consistent.

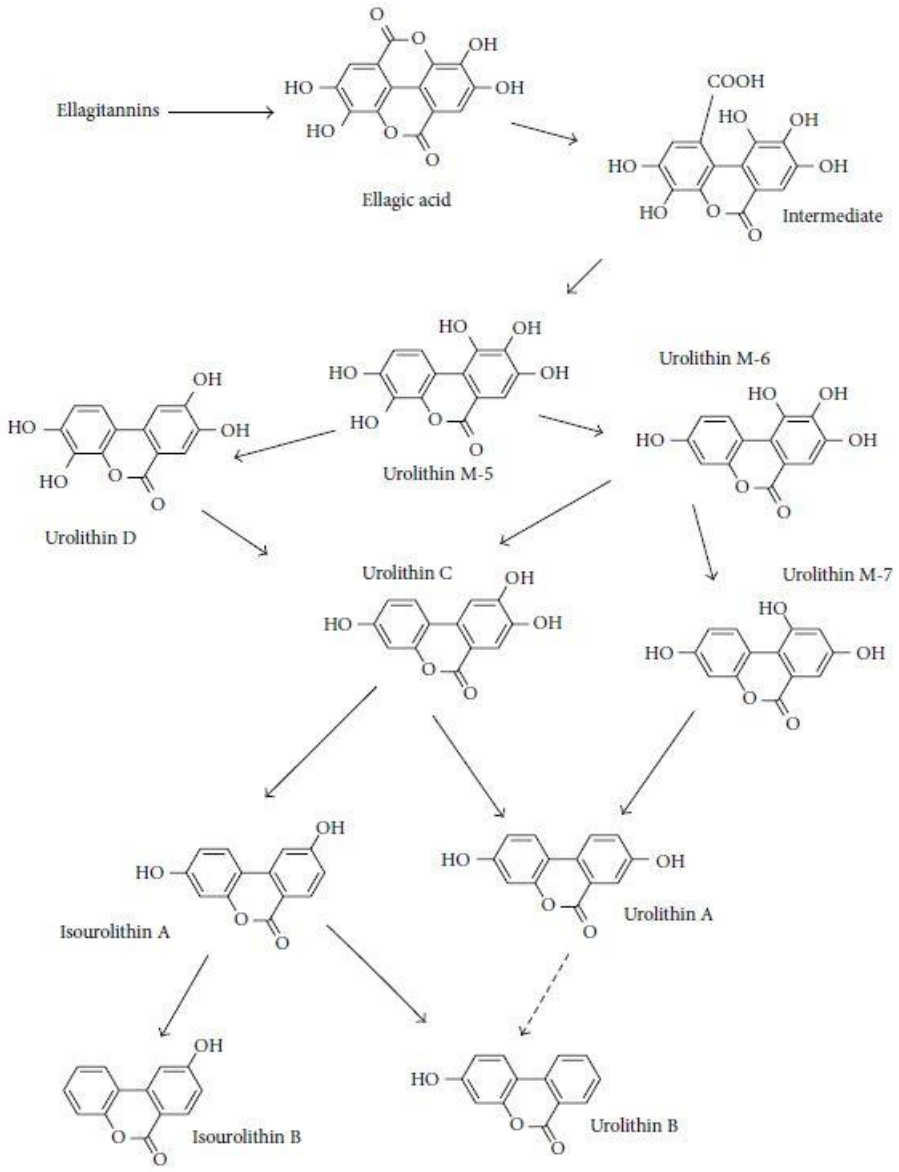

Figure 1: Step by step formation of urolithin A by microbial metabolization of ETs and EA taken from Espín et al. (2013).

Upon absorption, UroA quickly undergoes phase II metabolism with the major metabolites being glucuronide and sulfate conjugates, predominantly of UroA and UroB (Espín et al. 2013). Furthermore, it was found to pass enterohepatic circulation. In rodents, UroA was detected in colon and intestinal tissue as well as prostate and even brain tissue (Kujawska and Jodynis-Liebert 2020). Regarding human tissue, UroA could be found in prostates of patients suffering from prostate cancer or pathologically enlarged but not cancerous prostate glands, in its glucuronated form by González-Sarrías et al. (2010a), but also,

amongst others, in its free form in normal and malignant tissue of colorectal cancer (CRC) patients by Nuñez-Sánchez et al. (2014).

So far, UroA has mostly been associated with positive health effects. Heilman et al. (2017) concluded that the compound is neither genotoxic nor does it show any signs of neurological or reproductive toxicity in an animal study with Wistar rats. It was reported to display anti-oxidant, estrogenic, anti-carcinogenic and anti-inflammatory activity *in vitro* (Espín et al. 2013; Luca et al. 2020). As part of that, it acts anti-proliferative against cancerous cell lines of various organs like bladder, liver, prostate and colon carcinoma cells (González-Sarrías et al. 2014; Luca et al. 2020). UroA was reported to be capable of modulating certain signalling pathways or regulating enzymes involved in such (Kujawska and Jodynis-Liebert 2020). However, in which manner seems to be dependent on the experimental parameters as different studies show contrasting results. González-Sarrías et al. (2009a), for example, showed that UroA (40 µM) induced CYP1 enzyme activity in Caco-2 cells after 72 h assessed via 7-ethoxy-resorufin-*O*-deethylase (EROD) assay. Kasimsetty et al. (2010), on the other hand, found UroA (50 and 100 µM) to significantly diminish TCDD-induced CYP1 enzyme activity in HT-29 cells after 24 h. In another study, published by Muku et al. (2018), UroA diminished the purposely induced mRNA level of CYP1A1 in Caco-2 cells, partly achieved by competitive binding of the AhR, posing an antagonist of the receptor. This is affirmed by Singh et al. (2019) who revealed that CYP1A1 was one of the genes upregulated the most by UroA. They also found that UroA elevated mRNA levels of the TJPs Cldn4, Occl and ZO-1 in HT-29 cells as well as significantly enhanced the expression of Cldn4 and Occl. Furthermore, Singh et al. (2019) could show that the stimulation of TJP expression occurred in an AhR-Nrf2-dependent manner. Treatment with UroA also diminished LPS-induced leakage of FITC dextran in monolayers of HT-29 as well as Caco-2 colon carcinoma cells.

In vivo studies, mainly in rats, showed anti-inflammatory effects in animals suffering from ulcerative colitis as well as prebiotic effects by positively impacting gut microbiota composition which can further provide protection against inflammation (Espín et al. 2013). Another aspect of the anti-inflammatory properties of UroA is the reduction of pro-inflammatory mediators (Luca et al. 2020). Focusing on the correlation of inflammation in the intestinal environment with intestinal barrier function, UroA was able

to preserve mucosal and colonic architecture as well as attenuate destruction severity of the colonic epithelium in rats with inflammation induced by dextran sodium sulfate (DSS) (Larrosa et al. 2010). Singh et al. (2019) described UroA to enhance the barrier function by strengthening its integrity and exerting anti-inflammatory effects. Treatment ameliorated colitis in mice induced by DSS or 2,4,6-Trinitrobenzenesulfonic acid (TNBS) administration by counteracting barrier dysfunction and reduced serum levels of pro-inflammatory cytokines.

1.5 Mycotoxins

Certain fungi can compromise foodstuff, be it in our kitchen, the supermarket or our own little crop on the balcony. While only the moulds themselves are visible to the naked eye, some of them harbour a non-visible, additional threat: mycotoxins. These are part of the secondary metabolites produced by various species of fungi which often exert detrimental effects on humans and animals upon ingestion (Grenier and Applegate 2013).

Infestation of food commodities can occur still on the field as well as upon storage and lead to contamination with one or more toxins potentially persistent throughout various steps of food processing procedures (van Tran et al. 2020; Chen et al. 2021). About 25 % of yearly harvested crops worldwide is estimated to be contaminated with mycotoxins (Mishra et al. 2020). The main fungal genera concerning the formation of toxins in foodstuffs are *Aspergillus, Alternaria, Fusarium* and *Penicillium* (van Tran et al. 2020). One of the biggest problems with mycotoxins is their physicochemical stability enabling many of them to withstand even processing conditions, so their hazard is not only limited to raw material or hardly processed foodstuff (van Tran et al. 2020). The set-up of the present study included two different mycotoxins, deoxynivalenol (DON) and alternariol (AOH). One of them, DON, has been studied extensively over the last decades and counts to the most prominent mycotoxins globally observed (van Tran et al. 2020). The other one, AOH, belongs to the group of *Alternaria* toxins that gained growing attention over the last years and constitute so called “emerging mycotoxins” (Aichinger et al. 2021b). The term is used to describe novel mycotoxins for which no regulations have been established so far since

data on their toxicological profiles are yet insufficient for a comprehensive evaluation. (Gruber-Dorninger et al. 2017).

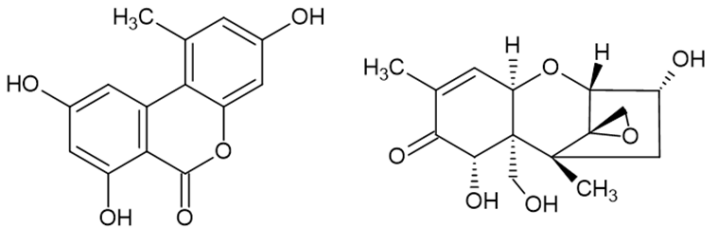

Figure 2: Chemical structures of the two mycotoxins alternariol (AOH) and deoxynivalenol (DON). The structures were drawn using the software ACD/ChemSketch.

1.5.1 Alternariol

Alternariol (AOH) is a mycotoxin produced by the fungal genus *Alternaria*, for instance *Alternaria alternata,* which belongs to the most commonly detected *Alternaria* species around the world, especially in products designated to human consumption (Chen et al. 2021; Lee et al. 2015a). *Alternaria* species were found to infest a number of crops with economic importance such as wheat, tomatoes and sunflower seeds (Chen et al. 2021). Furthermore, they were reported to be able to grow under low temperatures, posing an additional risk to foodstuff stored or transported at refrigerated conditions (Lee et al. 2015a). So far, more than 70 secondary metabolites with toxic properties produced by *Alternaria* were documented and are referred to as *Alternaria* toxins. Among the most prominent in fruits and vegetables are tenuazonic acid (TeA), altertoxin I (ATX-I), alternariol monomethyl ether (AME) and AOH (Chen et al. 2021). As of today, *Alternaria* toxins are regarded as emerging mycotoxins which occur frequently but are still unregulated (Gruber-Dorninger et al. 2017). However, the European Food Safety Authority (EFSA) recently published a recommendation for a more thorough monitoring of AOH as specified below. Importantly, AOH and its methylated derivative AME share similar properties and, for the most part, are stated collectively when discussed in terms of their effects and mechanisms. Hence, previous findings debated in this thesis can be assumed to most likely also be applicable to AME in addition to AOH. Chemically, AOH is a dibenzo-α-pyrone, its structure can be seen in Figure 2 (EFSA 2011). The toxin has been

detected in several food products like sunflower seed oil, wheat and barley but especially in tomato products and a variety of fruit juices (Fraeyman et al. 2017).

During phase I metabolism, hydroxylation of C-2, C-4 and C-8 were observed in human microsomes incubated with AOH (Pfeiffer et al. 2007). In terms of cellular uptake, oxidative stress, metabolism, topoisomerase inhibition and DNA damages the metabolite 4-hydroxy-alternariol (4-OH-AOH) exerted lower toxicity than AOH itself (Tiessen et al. 2017). Throughout phase II metabolism, mycotoxins often undergo conjugation, mostly with sulfate or glucose groups, favoured by phenolic hydroxy sites as does AOH (Solhaug et al. 2016b). These metabolization reactions can be realised by the fungi as well as by infested plant cells (Fraeyman et al. 2017). Consequently, many mycotoxins can be present in their pure form and as their conjugated metabolites simultaneously, referred to as “modified or masked mycotoxins”, which need to be considered for the assessment of the toxins amount as well as for analysis (Solhaug et al. 2016b; Aichinger et al. 2021b).

An exposure assessment of *Alternaria* toxins by EFSA (2016) estimated the human dietary exposure to AOH at 2.2 – 9.2 ng/kg(bw)/d which is considered to be rather low. The threshold of toxicological concern (TTC) for potentially genotoxic compounds by the EFSA Panel on Contaminants in the Food Chain (CONTAM Panel) is set to 2.5 ng/kg(bw)/d (EFSA 2011). According to these estimations, chronic AOH exposure predominantly exceeds the TTC. This was reinforced by Fan et al. (2021) conducting a biomonitoring study of *Alternaria* toxins (including AOH and AME) in human urine. Based on the urinary concentration the probable daily intake (PDI) was calculated. This revealed that, in samples where the respective mycotoxin was detected, 100 % (AOH) and 99.2 - 100 % (AME) of the participants’ PDIs exceeded the TTC. The toxicological hazard posed by these substances is therefore relevant in realistic scenarios.

The EFSA called for enhanced monitoring of *Alternaria* toxins and subsequent report and, in 2022, the European Commission published a recommendation following that (EFSA 2022). Therein they call for monitoring of AOH, AME and TeA in food with special focus on high-risk cohorts such as processed tomato products or cereal-based products for infants and children. They also advocate for a maximum LOQ when analytically determining AOH and AME set to 2 µg/kg for cereal-based foods for infants and young children and 4 µg/kg for other foods (EFSA 2022). Also, indicative concentrations are

stated for AOH, AME and TeA upon the exceeding of which further investigations for the cause of the higher prevalence are demanded.

Though acute toxicity of AOH is considered to be low, it has been reported to exert cytotoxic and genotoxic effects as well as being capable of interfering with reproductive systems *in vitro* (Solhaug et al. 2016b). In fact, susceptibility to the cytotoxicity of AOH was observed in several different mammalian cell lines leading to inhibited cell growth, induced apoptosis and restrained protein synthesis (Chen et al. 2021). With regard to the human organism, cytotoxicity seems to be strongly driven by oxidative stress, as was shown in a study by Fernández-Blanco et al. (2015) with Caco-2 cells in which AOH caused the formation of reactive oxygen species (ROS) and lipid peroxidation. As possible consequences of AOH's genotoxic properties, induction of gene locus mutations, chromosome aberrations and DNA damages or disordered DNA synthesis were reported, mainly *in vitro* (Chen et al. 2021). The latter was probably enabled due to its interaction with topoisomerases, increasing DNA strand breaks as observed in HT29 colon carcinoma cells by (Fehr et al. 2009). As mentioned above, AOH also intervenes with the hormonal balance as it can act as an endocrine disruptor due to its bi-phenolic structure that resembles the one of natural oestrogen (Solhaug et al. 2016b). Relating to structural characteristics, Dellafiora et al. (2018) investigated the impact of modifications on the oestrogenic activity of AOH and its emerging metabolites. Alkaline phosphatase assays revealed that methylation of AOH (as in AME) enhanced oestrogenic activity while glucuronidated and hydroxylated metabolites (like 4-OH-AOH) caused a reduction in oestrogenicity. While most research so far was limited to *in vitro* studies, there is also evidence for adverse effects *in vivo,* primarily focussing on the reproductive toxicity exerted by AOH e. g. concerning foetal weight in Syrian gold hamster (Chen et al. 2021) or embryo development in chicken (Escrivá et al. 2017).

Upon entering the intracellular compartment, the induction of ROS and the interaction with DNA topoisomerases appear to be the first targets or rather mechanisms of AOH (Fehr et al. 2009; Pahlke et al. 2016). The mycotoxin does not only act as an DNA topoisomerase I and II inhibitor, it also stabilizes the covalently bound complex of DNA and topoisomerase enhancing the risk for DNA double strand breaks (Fehr et al. 2009). One suggested way for the production of ROS by AOH is through its metabolization, in the

course of which it undergoes aromatic hydroxylation generating reactive catechols and hydroquinones which can further partake in the generation of ROS (Solhaug et al. 2016b). Such hydroxylation reactions are conducted by isoforms of the CYP enzyme family (van Tran et al. 2020). Interestingly, AOH, as well as AME, was found to be an activator of the AhR which acts as a transcription factor for the phase I metabolism enzyme CYP1A1 (Schreck et al. 2012). Therefore, it might promote its own metabolism further enhancing ROS production.

1.5.2 Deoxynivalenol

The mycotoxin deoxynivalenol (DON) is produced by *Fusarium* species such as *F. graminearum* and *F. culmorum* and belongs to the group of type B trichothecenes (Mishra et al. 2020). It is one of the most prevalent mycotoxins detected so far and was repeatedly reported to exert detrimental effects on human and animal health (EFSA 2017). Acute intoxication with DON in animals has been found to cause nausea, diarrhoea, decreased food intake and vomiting, which accounts for its trivial name "vomitoxin" (van de Walle et al. 2008). Besides, it might also be referred to as "ribotoxin". This term refers to DON interfering with protein translation and hence synthesis (Mishra et al. 2020). In more detail, DON binds to the peptidyl transferase of the 60S ribosomal subunit after uptake by the cells (van de Walle et al. 2010). The caused hindering of protein translation triggers ribotoxic stress and can further provoke the induction of the MAPK signalling pathway (Pinton et al. 2012). The infestation of foodstuff with *Fusarium* and thus DON is observable both on the field and under storage conditions (Mishra et al. 2020). Furthermore, as many other mycotoxins, DON constitutes a molecule that is stable under high temperatures occurring, for instance, during industrial processing or meal preparation and in milieus with a low pH value.

DON, although holding several hydroxy groups as can be seen in Figure 2, does not pose a substrate for phase I metabolism (van Tran et al. 2020). It is, however, diversely conjugated, mainly with sulfate groups or sugar moieties. The major human metabolites are found to be DON-15-glucuronide followed by DON-3-glucuronide, which, together with DON, are employed as biomarkers in human urine (EFSA 2017). Other metabolites of DON identified in humans are DON-3-glucoside, DON-7-glucuronide, DON-8-glucuronide

as well as the de-epoxylated DOM-1 which is formed by gut microbiota (van Tran et al. 2020). Warth et al. (2016) also identified a sulfated human metabolite of DON present in human urine, DON-3-sulfate (DON-3-Sulf; abbreviated “D3S” or “D-3-S” within the graphs).

Along the food chain, the commodities mainly contaminated by DON are grains and products thereof (EFSA 2017). However, it often co-occurs with modified DON metabolites, which in addition are largely broken down to “pure” DON upon ingestion (Mishra et al. 2020; EFSA 2017). Therefore, EFSA extended the assessed analyte from DON to a group consisting of DON, 3-acetyl-DON (3-Ac-DON), 15-acetyl-DON (15-Ac-DON) and DON-3-glucoside. In the course of an EFSA risk assessment from 2017 concerning DON and the three metabolites just mentioned, a mean acute exposure of 0.2 - 2.9 µg/kg (bw)/d and a mean chronic exposure of 0.2 – 2-0 µg/kg (bw)/d were estimated. Based on that, an acute reference dose (ARfD) of 8 µg/kg (bw) per eating occasion was postulated as well as a group tolerable daily intake (TDI) of 1 µg/kg (bw)/d (EFSA 2017).

Predominantly of interest for this thesis, is the effect DON can have on the intestinal epithelial barrier. The impact of mycotoxins on intestinal functionality was meta-analysed by Grenier and Applegate (2013). Some effects of DON have already been thoroughly studied, often showing dose dependence as in the studies of Springler et al. (2016), van de Walle et al. (2008) or Fernández-Blanco et al. (2016). Springler et al. (2016) observed reduced transepithelial electrical resistance (TEER) and a decline in the protein expression of Cldn1 and Cldn3, but not Cldn4, in differentiated IPEC-J2 cells after DON exposure. They further found that the effects on TEER and Cldn3 were also regulated via the same MAPK cascade. *In vitro* experiments in differentiated IPEC-1 cells by Pinton et al. (2010) demonstrated a reduction of Cldn4 protein expression, and consequently loss of barrier function, via MAPK activation. In Caco-2 cells, van de Walle et al. (2010) demonstrated an increase in mRNA transcription levels of the TJPs occludin (Occl) and Cldn4, a decrease of Cldn4 protein expression levels as well as increased permeability of a cell monolayer in terms of TEER values and flux of marker molecules caused by the mycotoxin. *In vivo,* Pinton et al. (2012) revealed that DON-contaminated feed caused histological alterations

in the jejunum of piglets, mostly in form of degeneration and fusion of villi, necrotic traces and in some places enterocyte lyses.

These exogenous compounds, however, can be subjected to biochemical modification and transformation, as mentioned before, which can have substantial impact on their efficacy. While the derivative 15-Ac-DON seems to be more toxic due to a high MAPK activation potential (Pinton et al. 2012), the human metabolite DON-3-Sulf and the microbial metabolite DOM-1 are considered to be detoxification products (Warth et al. 2016; Springler et al. 2016). Due to de-epoxidation, DOM-1 lacks the potential to inhibit protein translation as it cannot interact with the ribosome like DON (Springler et al. 2016). DON-3-Sulf also did not hinder protein translation or synthesis and, unlike DON, was not cytotoxic in SRB assays conducted in several human intestinal cell lines (Warth et al. 2016).

1.5.3 Co-Exposure

So far, the assessment of food contaminants focused mainly on the individual compounds (Crudo et al. 2019). However, natural food contaminants like mycotoxins can co-occur, for instance in a meal comprised by multiple ingredients of which several were contaminated individually. Pure foodstuffs themselves, however, are often impaired by multiple mycotoxins at once as well. On the one hand, they might be infested by more than one fungal species. *Alternaria* toxins, for one, were found to frequently occur alongside mycotoxins produced by other genera like *Fusarium* or *Penicillium* (Crudo et al. 2019). On the other hand, the infesting fungi could produce a whole variety of toxic compounds, which is often the case with *Alternaria,* to stick with this example, as was demonstrated by the biomonitoring study of Fan et al. (2021) mentioned earlier. Combined effects exerted by two compounds are characterized depending on the final outcome. An effect is considered “additive”, when the result of the mixture resembles the sum of the effects exerted by the individual compounds. “Synergism” describes a combinatory effect that exceeds the individual ones, while “antagonism” results in an effect weaker than additive (Chou 2006). Over the last years, more and more voices in the scientific community highlight the importance of co-exposure and hence possible combinatory effects of exogenous substances.

A study by Vejdovszky et al. (2016) revealed that TeA (10 µM – 200 µM) was able to attenuate the cytotoxic effect of 10 µM DON on Caco-2 cells in a WST-1 assay, exerting an antagonistic combinatory effect. Another study in Caco-2 cells investigated the effect of mycotoxin mixtures like AOH and DON on cell viability (Fernández-Blanco et al. 2016). Thereby, they observed mainly synergistic interactions upon 48 h and 72 h of incubation time with concentrations ranging from 3.1 µM – 30 µM for AOH and 0.625 µM – 5 µM for DON, respectively. Besides, mycotoxins can also interfere with non-toxic bioactive compounds present in the food matrix or *vice versa* (Crudo et al. 2019). Especially polyphenols, having various positive health benefits associated with them, are often subject to combinatory studies. For instance, the isoflavone genistein and the anthocyanidin delphinidin were able to protect HT-29 cells from genotoxicity induced by AOH (Aichinger et al. 2017), while pre-treatment with the flavonoid kaempferol mitigated detrimental effects of DON on differentiated Caco-2 cells by increasing TEER values as well as Cldn3 and ZO-1 protein expression (Wang et al. 2019).

1.6 Caco-2 *in vitro* Model

Over the last decades, *in vitro* studies have become more and more important, serving as pre-stage to clinical studies or to investigate certain mechanisms in their molecular detail. Additionally, the potential to reduce the amount of *in vivo* animal experimentation by developing evermore complex cell-based models eligible to replace them, gains importance (Ponce de León-Rodríguez et al. 2019). Further downsides of *in vivo* experiments, apart from the evident ethical issues, are their elevated costs, variations in sensitivities and hence responses due to interspecies differences and complications with extrapolating data gained in animals to the human organism (Ponce de León-Rodríguez et al. 2019). Besides, *in vitro* set-ups score with their high reproducibility and are suitable for high-throughput applications (van Tran et al. 2020).

For this study, the human colon carcinoma cell line Caco-2 C2BBe1 (clone CRL2102 after ATCC) was chosen. It is one of the most commonly used, and therefore best characterized, cell lines when it comes to research questions regarding the intestinal environment (van de Walle et al. 2010). Although it is a cancerous cell line, it is well applicable for studies mimicking a healthy intestinal epithelium as it expresses characteristics of normal

intestinal cells after differentiation which occurs spontaneously upon confluency (Ponce de León-Rodríguez et al. 2019). These include the formation of a brush border layer with respective enzymes, membrane transporters similar to those of enterocytes and, most notably, tight junctions, substantially mimicking the intestinal *in vivo* barrier (van Tran et al. 2020; van de Walle et al. 2010). Therefore, monolayers of Caco-2 cells are often utilized to investigate aspects like permeability, metabolism, bioavailability as well as transepithelial transport (van Tran et al. 2020).

1.7 Aim of this Thesis

In consideration of all the outlined issues and their potential to co-occur, the aim of this study was to elucidate their implication on the colonic intestinal epithelial barrier integrity. Therefore, the following questions were posed:

- What are the impacts of exposure to the two food contaminating mycotoxins AOH and DON on the epithelial integrity *in vitro*?
- What kind of impact does the food-related gut microbial metabolite UroA exert on the colonic epithelium?
- In what way could tight junction proteins such as ZO-1 be involved in the respective effects?
- Could the AhR pathway participate in the effects toward the intestinal epithelium?
- Are there any interactions upon binary exposure to the three substances regarding the outcomes observed for single treatment?
- Does pre-existing or concurring inflammation influence the efficacy of the food-derived substances at the intestinal epithelium?

2 Materials and Methods

2.1 Chemicals and Consumables/Materials

Dulbecco's Modified Eagle Medium (DMEM), additives, DPBS and Pierce™ Bicinchoninic Acid Protein Assay Kit were obtained from Gibco Thermo Fisher Scientific (Waltham, MA, USA). General labware for cell culture maintenance and experiments was purchased from Sarstedt AG & CO (Nuembrecht, Germany), slides for imaging were obtained from Ibidi (Graefeling, Germany). DON was acquired from Romer Labs (Tulln, Austria), DMSO and Triton X-100 from Carl Roth (Karlsruhe, Germany). AOH, UroA, CH223191, Benzo-{*a*}-pyrene (B[a]P), resorufin ethyl ether (7-ER), resorufin, dicoumarol, bovine serum albumin fraction V (BSA), Neutral red dye (NR) and Lucifer Yellow CH dilithium salt (LY) were purchased from Sigma Aldrich Chemie GmbH & Co (Steinheim, Germany). Human IL-1β was obtained from InvivoGen (Toulouse, France). Primary antibodies for fluorescence imaging ZO-1 (goat; ab190085) and CYP1A1 (rabbit; ab235185) were acquired from Abcam (Cambridge, UK), primary antibody α-tubulin (mouse; sc-5286) and secondary antibodies donkey anti-mouse 488, donkey anti-rabbit 568 and donkey anti-goat 647 from Santa Cruz (Heidelberg, Germany). Stock solutions were prepared in ddH_2O or DMSO, respectively.

Plates and inserts from two different manufacturers, Sarstedt AG & CO (Nuembrecht, Germany) and Corning Incorporated Life Sciences (Lowell, MA, USA), were used for permeability assays. Corning trademarked the term Transwell® for labware suitable for such experiments, while Sarstedt refers to their inserts etc. as tissue culture (TC) inserts. For reasons of simplification, the abbreviation TW (Transwell) will be used for equipment allowing two-compartment *in vitro* set-ups in general, independently of the manufacturer.

2.2 Cell Culture

Human adenocarcinoma Caco-2 C2BBe1 cells (clone CRL2102 after ATCC) obtained from ATCC (Manassas, VA, United States) were subcultured in DMEM with 10 % foetal calf serum (FCS), 1 % (v/v) penicillin/streptomycin (100 U/mL each), 1% (v/v) sodium pyruvate and 0.01 mg/mL human insulin-transferrin-selenium as previously described by Schmutz et al. (2019) or Beisl et al. (2021). They were incubated at 37 °C in a humified atmosphere

with 5 % CO_2. Cells were split upon 70-80 % confluency twice a week. For experiments, they were seeded in required plates and incubated under the same conditions. Medium was refreshed every two to three days. Only cells with a passage number below 30 were used to conduct this study.

Substance treatment (for 24 h or 48 h) started seven days after seeding since by then the cells differentiated and formed a coherent monolayer (Figure 3; (Hidalgo et al. 1989). Eventual concentrations of the three substances of interest were elected ensuing testing concentration ranges for their cytotoxicity (Figure 4) and resulted in UroA (25 µM), AOH (25 µM) and DON (2.5 µM). The final incubation solutions were composed of DMEM medium supplemented as stated before, the respective amount of testing substance and a total DMSO concentration of 1.1 % each, since some compounds were dissolved in DMSO. Where applicable, IL-1β was added with a concentration of 25 ng/ml.

If not indicated otherwise, experiments were performed with a biological replicate of n ≥ 5 comprising a technical replicate of n = 3 each.

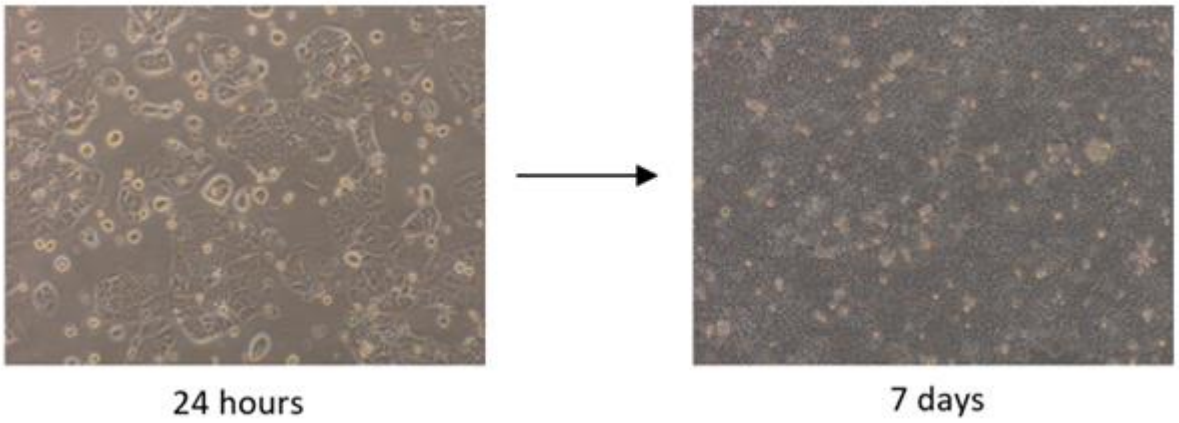

Figure 3: Microscopy images of Caco-2 cells let grown beyond confluency and differentiate for seven days after seeding. Pictures were taken with an Olympus camera at 10 X magnification. Product version: OLYMPUS cellSens Entry 1.18 (Build 16686).

2.3 Neutral Red (NR) Cytotoxicity Assay

To assess cell viability under the applied conditions, a Neutral Red (NR) assay was performed. Prerequisite for this experiment is the ability of viable cells to take up and accumulate the NR dye into their lysosomes (Repetto et al. 2008). The dye is then

extracted from the cells and its concentration determined photometrically via absorbance measurements.

First, cells were seeded in 96-well-plates at a density of 85.000 cells/cm² (24.650 cells per well). One row was filled with phosphate-buffered saline (PBS) to serve as blank. The cells were differentiated for seven days under the conditions stated above (Chapter 2.2) before performing the assay. Subsequently, culture medium was exchanged for incubation solutions and, in case of measurements performed in presence of pro-inflammatory stimulus, IL-1β was added 2 h afterwards. Since NR is a photosensitive dye, the assay was conducted in the dark or under infrared (IR) light. On the day before the assay was conducted, a 1:100 dilution of a NR stock (4 mg/ml NR dye in DPBS) in culture medium (supplemented DMEM) was prepared and equilibrated overnight to incubation conditions. Immediately before the assay, this NR medium was centrifuged for 15 min at 600 rpm to accumulate possible precipitation and the supernatant was filtered. The incubation medium was removed from the plate, 100 µl NR filtrate were added to each well and incubated for 2.5 h at 37 °C. Afterwards, the NR medium was discarded, the plate was washed with prewarmed DPBS and 150 µl/well destaining solution were applied, consisting of 50 % ethanol absolute, 50 % ddH_2O and an additional 1 % of glacial acetic acid. The plate was put on a shaker for 10 min at just under 500 rot/min. Subsequently, 130 µl of the supernatant were transferred to a fresh transparent 96-well-plate and absorbance was measured at 540 nm using a plate reader (BioTek CytationTM 5 Multi Mode Reader; Agilent Technologies, Santa Clara, CA, United States).

2.4 Enzyme Activity

To investigate the activity of several isoforms of CYP enzymes family 1 (CYP1A1, CYP1A2 and CYP1B1), the EROD assay (see chapter 2.4.1) was chosen. A bicinchoninic acid (BCA) assay (see chapter 2.4.2) to determine the total protein content was performed in addition to correlate enzyme activity to the same protein content within all samples. The established, high-affinity, AhR ligand B[a]P (1 and 5 µM) was used as positive control, the reportedly full AhR antagonist CH223191 (5 µM) as indirect “negative” control (Zhao et al. 2010). Correspondent to previous experiments at the institute (Hohenbichler et al. 2020;

Pahlke et al. 2016), preliminary tests with varying concentrations and incubation times were run to settle on those subsequently described. Based on Schiwy et al. (2015), the resulting enzyme activity was calculated using the following Equation 1.

$$enzyme\ activity = \frac{c\ (resorufin)[nM]}{30\ \cdot c\ (protein)[mg/ml]}$$

Equation 1

2.4.1 7-Ethoxy-Resorufin-*O*-Deethylase (EROD) Assay

Differentiated Caco-2 cells, that were treated with the substances of interest for 48 h, were incubated with EROD medium (colourless DMEM with 10 µM dicoumarol and 10 µM 7-ER) for exactly 30 min at 37 °C. The supernatant was aspirated to stop the reaction and the cells were washed (DPBS) and stored at -80 °C immediately. 75 µl of the supernatant were then transferred to a black 96-well-plate pre-filled with 200 µl absolute ethanol, EROD medium was used as blank and fluorescence was measured at 595 nm_{em}/535 nm_{ex} using a plate reader (BioTek CytationTM 5 Multi Mode Reader). The concentration of resorufin, for the correct calculation of enzyme activity, was determined via external calibration using resorufin stock solutions.

2.4.2 Bicinchoninic Acid (BCA) Assay

The EROD plates stored at -80 °C were subjected to at least three thaw-freeze-cycles alternating between room temperature (RT) and -80 °C for at least 30 min each to lyse the cells. The cells were checked for lysis using the light microscope, all further steps were performed on ice. DPBS was added to each well and the cells were scraped off the surface using a pipette tip. The suspensions were centrifuged in pre-cooled Eppis at 4 °C with 14 000 rpm for 20 min. Subsequently, the supernatants were diluted 1:10 in ddH_2O and incubated in a clear 96-well-plate with BCA working reagent (ratio 50:1 of reagents A:B included in the kit) for 30 min at 37 °C. Following this, the absorbance was measured at 562 nm using a plate reader (BioTek CytationTM 5 Multi Mode Reader) and the total protein content was determined via a simultaneously measured BSA calibration curve.

2.5 Immunofluorescence (IF) Staining

The cells were seeded and differentiated in 8-well µ-slides (Ibidi) as described above. After an incubation time of 48 h with the respective substances, immunofluorescence staining based on established protocols of the institute was performed (Beisl et al. 2021; Del Favero et al. 2018; Groestlinger et al. 2022b). Accordingly, the cells were fixed with 3.7 % formaldehyde (FA) and washed with PBS-A. Permeabilization was conducted with 0.2 % Triton X-100 and subsequently unspecific binding sites were blocked using 1 % BSA (in PBS-A). Afterwards, primary antibodies were applied to the cells for 2 h. After three washing steps with 0.05 % Triton X-100 à 10 min and one washing step with PBS-A à 5 min, secondary antibodies were applied for 1.5 h. Following another three washing steps with 0.05 % Triton X-100 and three with PBS-A, post-fixation of the antibodies for 10 min was performed using 3.7 % FA. Subsequently, the cells were washed with PBS-A, quenched using a 100 mM glycine solution for 5 min, washed again with PBS-A and finally covered with mounting media (ROTI Mount DAPI (Abcam)). The slides were put on a shaker for all incubation steps.

Blinded imaging (by the supervisor) was conducted with a LSM Zeiss R 710 microscope coupled to an ELYRA PS.1 system, equipped with an AndoriXon 897 (EMCCD) camera and a Plan Apochromat 63X objective. At least five regions of interest (ROI) were randomly chosen per well. Image analysis determined the fluorescence intensity per ROI for each of the four different channels, respectively, and was performed using Zeiss Imaging and Analysis software ZEN (black edition). The obtained fluorescence intensities were then referred to the solvent control which was set to 100 %. Four biological replicates were acquired and analysed.

2.5.1 Preparation of IF Staining Solutions

All dilutions of TX-100 (0.2 % and 0.05 %), BSA (1 % and 0.25 %) and FA (3.7 %) were prepared in PBS-A. Primary antibodies were diluted 1:250 and secondary antibodies 1:1000 in 0.25 % BSA. The 100 mM glycine solution for quenching was also prepared with PBS-A. The upfront prepared PBS-A consisted of 0.4 g KH2PO4, 0.4 g KCl, 16 g NaCl and 5.5 g Na2HPO4 · 2 H_2O dissolved in 1000 ml ddH_2O, set to a pH of 7.2 and sterilised.

2.6 Permeability Assays

2.6.1 Transepithelial Electrical Resistance (TEER) Measurement

Cells were seeded in 12-well TW plates (Corning®) at a density of 85.000 cells/cm² (95.200 cells per well) on the apical side of the insert (0.4 µm pore size) in 500 µl medium compounded as stated above. The basolateral chamber was filled with 1500 µl medium. The TEER was taken at three different sites of the inserts, representing the technical replicates in the case of the TW plates. The TEER was measured five days after seeding, immediately before substance incubation (after seven days of differentiation) and 24 h as well as 48 h upon treatment using a voltohmmeter.

To establish the method for two new types of inserts (Sarstedt inserts “translucent” and “transparent”), an attempted daily measurement of the TEER of two biological replicates over a period of 21 days upon seeding was conducted preliminary to the experiments (see Supplementary Experiments, Suppl. Figure 1).

2.6.2 Lucifer Yellow (LY) Assay

Following the TEER measurements, a Lucifer Yellow (LY) assay was performed to investigate the monolayer’s permeability to the passage of small molecules. Therefore, the medium in the TW plates was removed, the compartments were washed and 500 µl Lucifer Yellow solution as well as 1500 µl HBSS buffer were applied to the apical and basolateral chamber, respectively. After 1 h of incubation, the permeated amount of LY was obtained by determining the concentration of LY within the medium in the basolateral compartment by measuring the fluorescence at 485 nm_{ex}/535 nm_{em} using a plate reader (BioTek CytationTM 5 Multi Mode Reader). The contents of the apical and basolateral chambers were stored in opaque Eppis at -80 °C for further analysis as well as the plates now containing only cells without any liquid.

2.7 Statistical Analysis

Raw data were organised, summarised and pretreated using Microsoft Excel (Version 2210). Outliers were determined via Nalimov test. The software OriginPro 2021b was employed for further statistical analysis.

3 Results

3.1 Cell Viability/Cytotoxicity

NR assays, assessing the lysosomal activity of cells, were performed to exclude possible interferences by toxic effects of the test compounds towards the cell line in various other biochemical and biophysical experiments. All substances applied in the experimental set-up of the study were tested in a dose-range including the respective concentrations (Figure 4, Suppl. Figure 2). The initial NR data obtained for the main substances of interest (AOH, DON, UroA) for 24 h incubation time with IL-1β stimulation were complemented by data recently published by Groestlinger et al. (2022a). Only incubation conditions involving DON in an inflammatory state showed significant detrimental effects on the cells' lysosomal content, hence viability, after 48 h (Figure 5). The non-ionic surfactant Triton-X 100 (diluted 1:1000) was utilised to lyse the cells und thus served as "cytotoxic" control. It reduced cell viability to < 1 % (Suppl. Figure 2B and C, Figure 5).

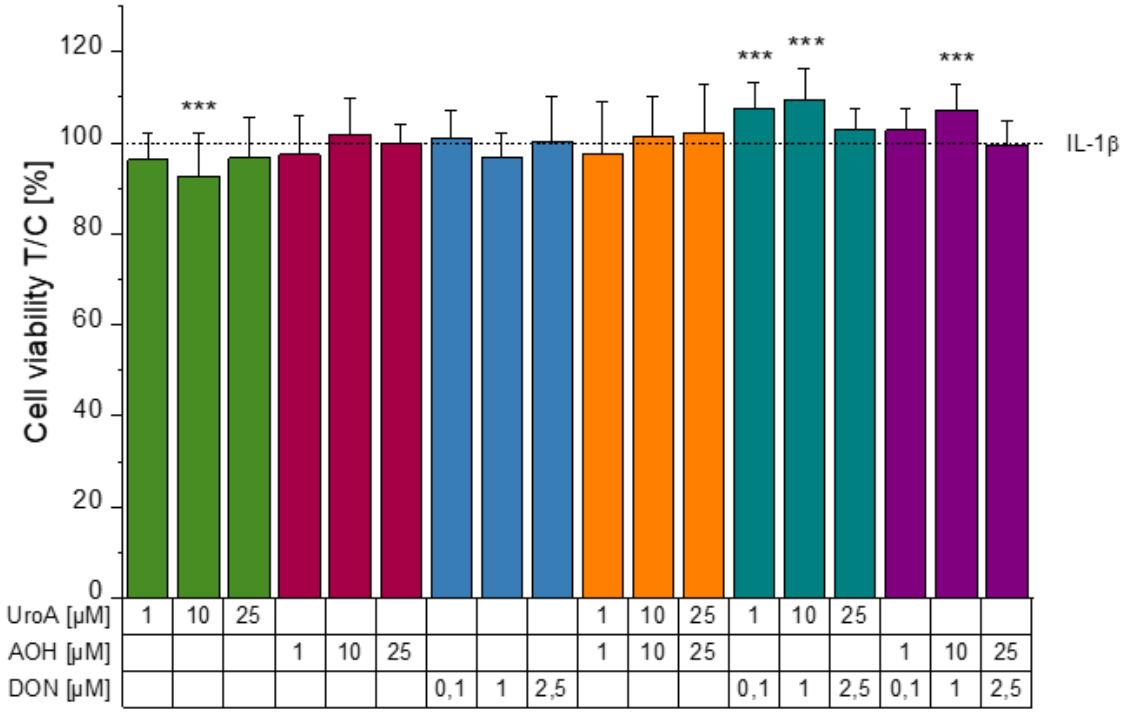

*Figure 4: Neutral red assay in Caco-2 cells (stimulated with IL-1β 2 h upon substance incubation) after 24 h incubation time. Cell viability determined as lysosomal activity was normalised against IL-1β solvent control and is plotted as percentage (T/C). A two-sample Students' t-test was applied to calculate significant differences compared to the solvent control which are shown as * (p<0.05), ** (p<0.01) and *** (p<0.001).*

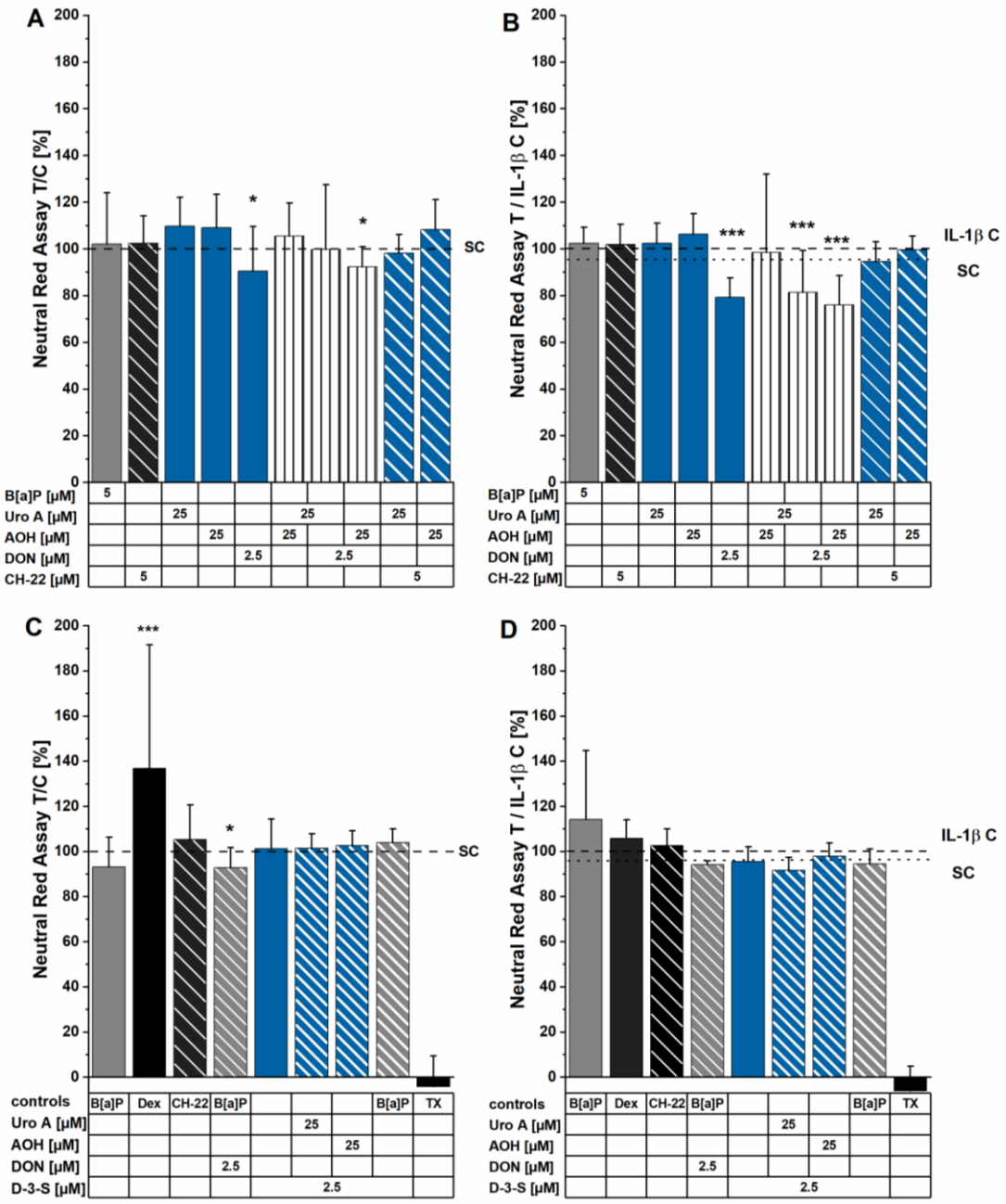

*Figure 5: Neutral Red data, taken from Groestlinger et al. (2022a), for an incubation time of 48 h without inflammatory stimulus (A, C) and with IL-1ß stimulus (B, D) 2 h after incubation start. Measurement results were normalised against DMSO solvent control (SC) or IL-1ß solvent control and are depicted as percentage (T/C). Applied concentrations not stated in the figure for C) and D) are: B[a]P (1 µM), Dex (5 µM) and CH-22 (5 µM). The abbreviation "D-3-S" is equivalent to "D3S" as well as "DON-3-Sulf". Two-sample Students' t-tests were applied to calculate significant differences compared to the respective solvent control which are shown as * (p<0.05), ** (p<0.01) and *** (p<0.001).*

3.2 Examination of AhR Involvement in the Regulation of Barrier Integrity

3.2.1 Enzyme Activity of CYP1A1, CYP1A2 and CYP1B1

Regulation of GIT homeostasis is crucial for intestinal health. A disbalance thereof can, amongst other consequences, have detrimental effects on the mucosal barrier (Gao et al. 2020). Induction of the AhR is linked to barrier function and often reported to reinforce challenged epithelial integrity (Yu et al. 2018). As the AhR functions as a transcription factor for a group of CYP enzymes, the EROD assay assessing the enzyme activity of CYP1A1, CYP1A2 and CYP1B1 (Donato 1993; Iwata et al. 2015) was applied to determine the activation of the AhR signalling pathway caused by the compounds of interest.

The two dibenzo-α-pyrones AOH and UroA revealed to have an inducing effect on the EROD enzyme activity assessing P450 enzymes regulated by the AhR, while DON caused a slight decrease in activity (Figure 6A). Co-exposure to AOH and UroA resulted in an enzyme activity at the level of AOH alone, exceeding that of UroA alone (Figure 7). Interestingly, when AOH or UroA where applied in combination with DON, no effect on enzyme activity beyond the basal level was observed. Further, the hypothesis whether the observed restraining effect of DON was attributable to its protein synthesis inhibiting mechanism of action was examined (van de Walle et al. 2010). On that account, DON was compared to its (human) metabolite DON-3-Sulf which reportedly does not interfere with protein synthesis (Warth et al. 2016). As can be seen in Figure 6A, DON-3-Sulf did not hinder the induction caused by AOH and UroA as DON.

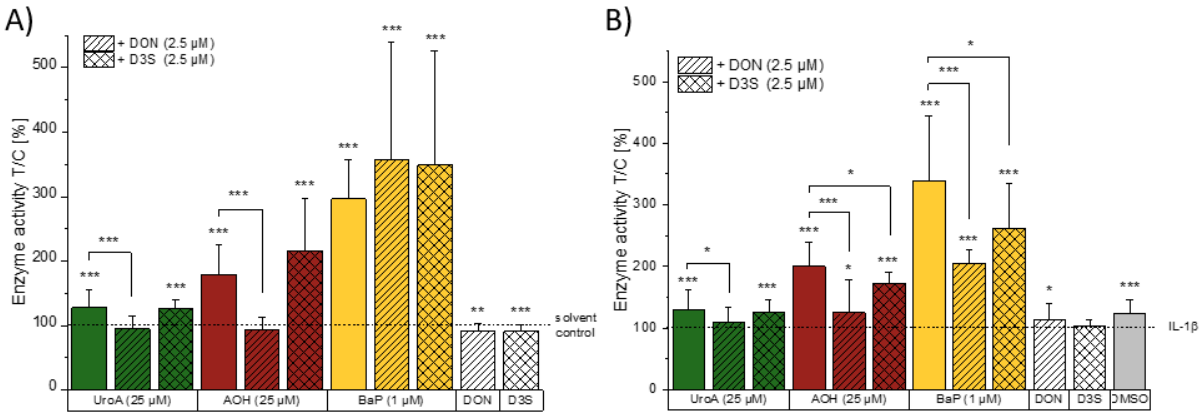

*Figure 6: Enzyme activity (EROD assay) of Caco-2 cells after 48 h of substance incubation without (A) and with (B) IL-1β stimulation after 2 h. Measured activity was normalised against A) DMSO solvent control and B) IL-1β control, respectively, and expressed as percentage (T/C). "D3S" is equivalent to DON-3-Sulf in the text. Two-sample Students' t-tests were applied to calculate significant differences compared to the respective control which are shown as * (p<0.05), ** (p<0.01) and *** (p<0.001).*

The same conditions were applied to cells additionally challenged with the pro-inflammatory cytokine IL-1β (Figure 6B). The effect of the individual compounds resembled those in the non-inflammatory state (Figure 6). The enhanced enzyme activity by UroA, AOH and B[a]P was decreased by co-incubation with DON. Interestingly, in this scenario the metabolite DON-3-Sulf also had a diminishing impact on the effect of AOH as well as B[a]P, however not to the extent of DON.

Referring the IL-1β stimulated conditions to the non-stimulated solvent control revealed a reduced effect for UroA in the stimulated state (Suppl. Figure 4), but in general the trends remained. Looking at the relation to the solvent control of an inflammatory environment (IL-1β), inflammation seems to have an influence on the induction of the enzymes CYP1A1, CYP1A2 and CYP1B1.

To test, whether the enzyme induction by AOH and UroA was AhR-dependent, the antagonistic CH223191 was co-incubated with both compounds, respectively. Figure 7 clearly shows that the enzyme activity inducing capacity of both testing compounds could not be observed when AhR was inhibited, demonstrating its necessity for the mechanism of action of AOH and UroA. No differences were observed when comparing the IL-1β stimulated to the non-stimulated condition. Hence, enzymatic induction caused by UroA and AOH, respectively, was hindered by CH223191 in presence or absence of the pro-inflammatory cytokine, as depicted in Figure 7A and B.

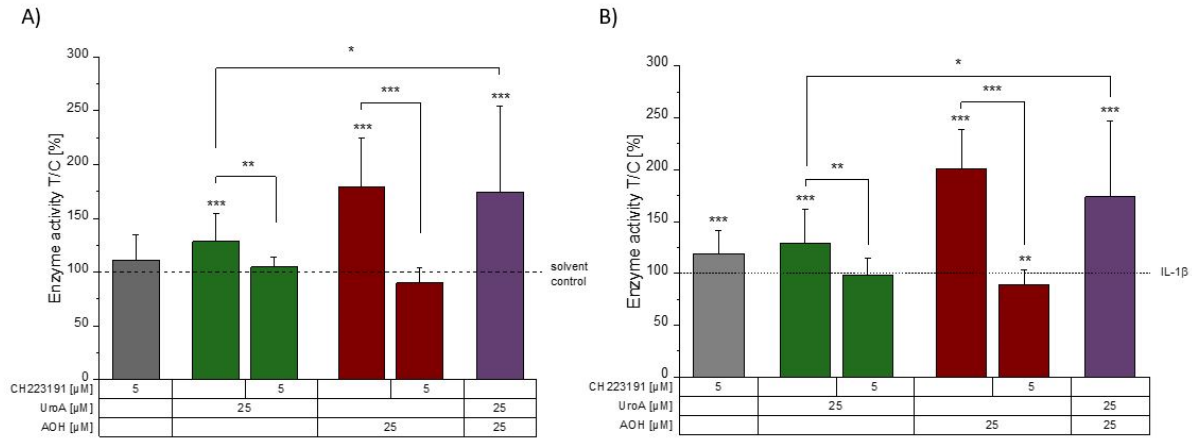

*Figure 7: Enzyme activity (EROD assay) of Caco-2 cells after 48 h without (A) and with IL-1ß stimulation (B) 2 h into incubation. Cells were (co-)incubated with CH223191, an antagonist of the AhR which represents a transcription factor for the assessed enzymes. Results were normalised against the respective solvent control and depicted as percentage (T/C). A two-sample Students' t-test was applied to calculate significant differences compared to the solvent control which are shown as * (p<0.05), ** (p<0.01) and *** (p<0.001).*

3.2.2 BCA Assay

The results of the BCA assay, conducted to normalize enzyme activity assessed via the EROD assay, were plotted separately to gain additional insight in possible cytotoxic effects of the substances in use on the applied cell model. Total protein content of cells exposed to an inflammatory stimulus (IL-1β) appears to be more affected compared to the same treatment in a non-inflammatory environment, as depicted in Figure 8B and Figure 8A, respectively. Incubation with DON alone, as well as in combination with AOH or UroA, led to a significant decrease in total protein content of cells additionally challenged with IL-1β. This does not only reflect the protein synthesis inhibiting mechanism of action of DON, but also matches the results of the NR assay, which showed a more reducing effect on cell viability, in terms of lysosomal activity, by DON when applied in an inflammatory environment (Figure 5B).

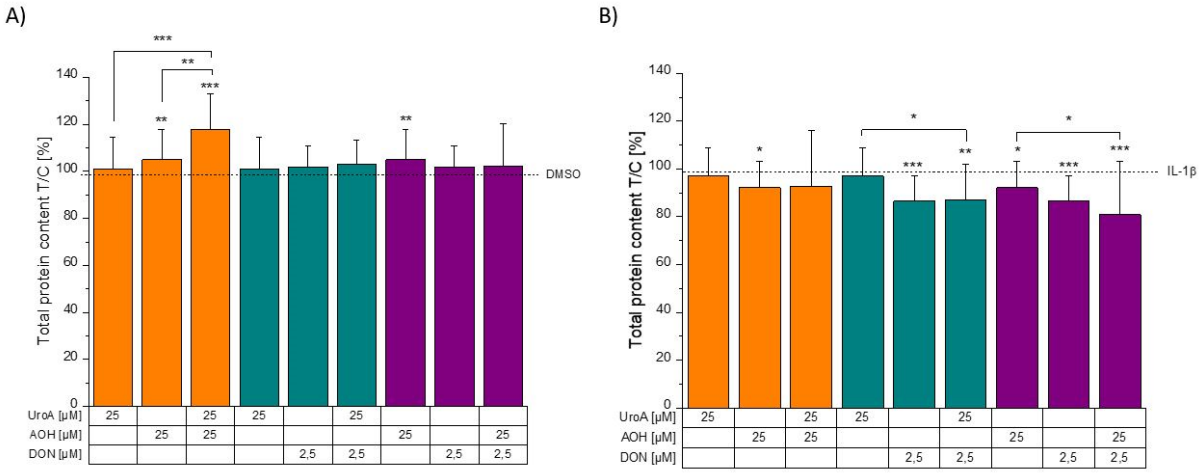

*Figure 8: Total protein content gained employing a BCA assay after treatment for 48 h A) without and B) with inflammatory stimulus (IL-1β). Results are expressed as percentage (T/C) after normalisation against the respective solvent control. A two-sample Students' t-test was applied to calculate significant differences compared to the solvent control or between selected conditions which are shown as * (p<0.05), ** (p<0.01) and *** (p<0.001).*

3.2.3 Immunofluorescence Staining of CYP1A1

To complement the analyses of the enzyme activity, CYP1A1-specific antibodies were included in the cell imaging experiments to assess the enzymes abundance on protein level. Since CYP1A1 is one of the main enzymes whose transcription is regulated by the AhR (Lamas et al. 2018), this could provide further insight about a possible participation of the AhR but also specify the involvement of the enzymes assessed collectively by the

EROD assay. Incubation with the single substances revealed a decline in CYP1A1 concentration (based on fluorescence signal intensity) for DON and AOH (Figure 9). No significant change was observed for UroA. Regarding binary treatments, the diminishing effect towards CYP1A1 immunofluorescence signals of both mycotoxins was counteracted respectively by the combination with UroA. Interestingly, co-incubation of AOH with DON showed the same effect, opposing to the effect of the individual compounds.

To additionally examine the involvement of the AhR, AOH and UroA were co-incubated with CH223191, retracing the layout of the EROD experiments. In the case of AOH, this resulted in a significantly increased signal compared to exposure to the dibenzo-α-pyrone alone (Figure 9). B[a]P (5 µM) was used as positive control and enhanced CYP1A1 presence within the cells.

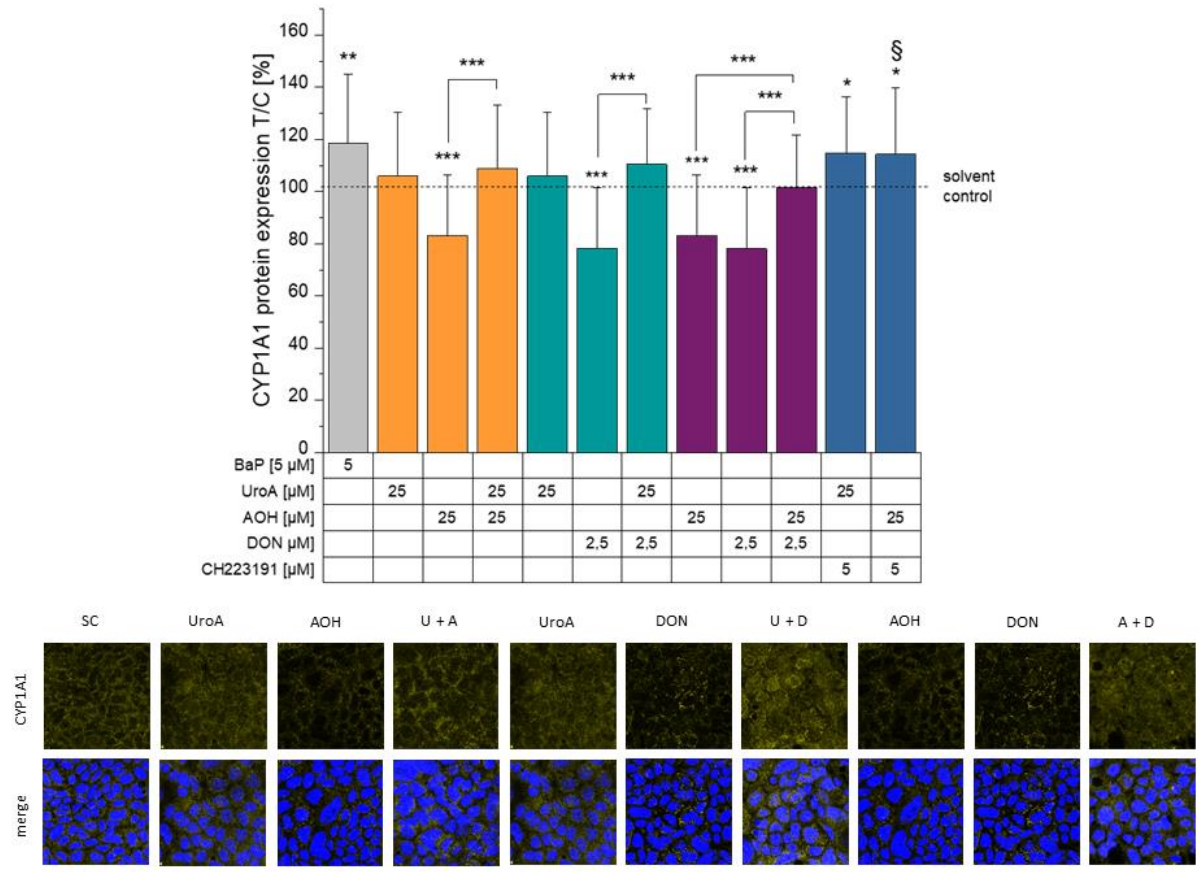

*Figure 9: Protein expression of CYP1A1 in differentiated Caco-2 cells after 48 h of substance treatment. Assessment was conducted by means of fluorescence intensity after image analysis of the immunofluorescence (IF) staining, normalised to the DMSO solvent control and expressed as percentage (T/C). Two-sample Students' t-tests were applied to calculate significant differences compared to the solvent control which are shown as * ($p<0.05$), ** ($p<0.01$) and *** ($p<0.001$). § marks significant differences of binary treatments with CH223191 to the respective second compound with ($p<0.01$). The images shown depict representative examples. The immunofluorescence signal related to CYP1A1 is displayed in yellow, "merge" shows CYP1A1 plus the nuclei in blue; A = AOH, D = DON, SC = solvent control, U = UroA.*

3.3 Barrier Integrity and Permeability of the Epithelial Cell Monolayer

Due to difficulties concerning the equipment, the initially performed replicates of the TEER and LY measurements turned out not to be reliable for further analysis. The TEER and LY data presented below were therefore acquired posterior by the supervisor.

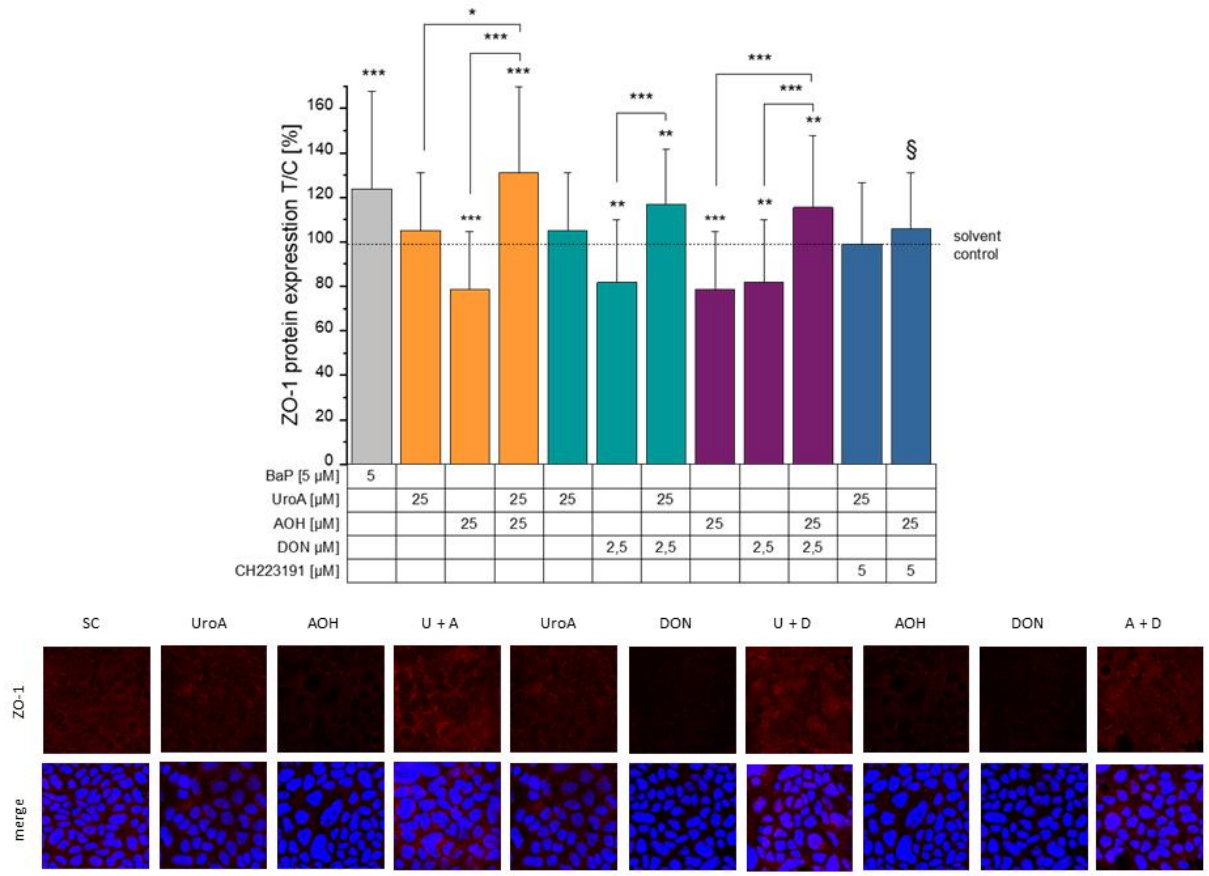

*Figure 10: Protein expression of ZO-1 in differentiated Caco-2 cells after 48 h of substance treatment. Assessment was conducted by means of fluorescence intensity after image analysis of the immunofluorescence (IF) staining, normalised to the DMSO solvent control and expressed as percentage (T/C). Two-sample Students' t-tests were applied to calculate significant differences compared to the solvent control which are shown as * ($p<0.05$), ** ($p<0.01$) and *** ($p<0.001$). § marks significant differences of binary treatments with CH223191 to the respective second compound with ($p<0.01$). The images shown depict representative examples. The immunofluorescence signal related to ZO-1 is displayed in red, "merge" shows ZO-1 plus the nuclei in blue; A = AOH, D = DON, SC = solvent control, U = UroA.*

3.3.1 Immunofluorescence (IF) Staining of ZO-1

Since the sealing and thus the permeability of the epithelium is mainly regulated via tight junctions (Gao et al. 2020), experiments investigating whether any alterations on protein level would be observable upon treatment with the tested substances were carried out. Therefore, the TJP ZO-1 was included in the IF staining set-up. UroA showed no

(pronounced) effect on the fluorescence intensity corresponding to ZO-1, while DON caused a decrease compared to the solvent control (Figure 10). Treatment with AOH also led to a reduced occurrence of ZO-1.

After dual co-exposure to the three main components, the epithelial monolayer responded with an increased expression of ZO-1 in all three scenarios (Figure 10). This is interesting, as there is one compound impairing this aspect in every mixture and no single substance caused an increase above solvent control level. The combination of UroA and DON led to a significantly higher ZO-1 expression than DON alone. The pairing of UroA and AOH exceeded the expression levels of both single compound treatments. Intriguingly, co-treatment with the two mycotoxins also resulted in a significantly increased expression of ZO-1, despite the reducing effects of both compounds individually. B[a]P (5 µM) was again used as positive control and enhanced ZO-1 presence, also apparent in Figure 10.

3.3.2 Immunofluorescence Staining of α-Tubulin

The cytoskeletal scaffold protein α-tubulin was also included in the immunofluorescence experiment to visualise possible impacts on the cytoskeleton, which could also potentially account for a loss of morphology and change barrier permeability. DON, as single substance as well as in combination with AOH, had a declining effect on the overall abundance of α-tubulin in the cells. While UroA alone showed no significant effect, it led to an increased signal when co-incubated with AOH (Figure 11). Combining UroA with DON however, resulted in a lower expression of α-tubulin than UroA alone. Since TJPs are closely intertwined and interact with the cytoskeleton, disruption of which also reduces the intestinal epithelial barrier function, the effects of blebbistatin (Blebb) and cytochalasin D (CytD) were tested as well (Le Shen et al. 2011). The two substances are drugs known to target crucial constitutes of the cytoskeletal network and were included to check whether one of them would be applicable as positive control for the detrimental effect on the cells protein scaffold (Ho et al. 2019; Jalimarada et al. 2009). Neither of these substances showed the anticipated effects, when regarding all three different staining endpoints (Suppl. Figure 3), however, the cells seem to respond more sensitively to CytD than to Blebb at the same concentrations. Treatment with B[a]P, albeit showing marked deviation, led to increased immunofluorescence signal of α-tubulin (Figure 11).

Furthermore, co-treatment with AOH and CH223191 enhanced the protein expression of α-tubulin compared to AOH alone, other than UroA (Figure 11).

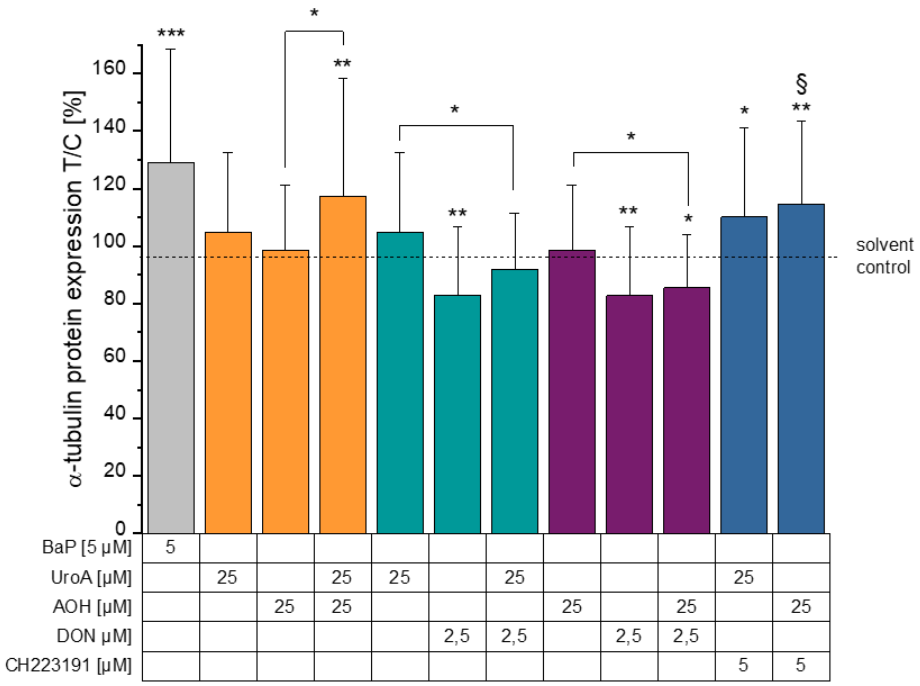

*Figure 11: Protein expression of α-tubulin in differentiated Caco-2 cells after 48 h of substance treatment. Assessment was conducted by means of fluorescence intensity after image analysis of the immunofluorescence (IF) staining, normalised to the DMSO solvent control and expressed as percentage (T/C). Two-sample Students' t-tests were applied to calculate significant differences compared to the solvent control which are shown as * (p<0.05), ** (p<0.01) and *** (p<0.001). § marks significant differences of binary treatments with CH223191 to the respective second compound with (p<0.05).*

3.3.3 Transepithelial Electrical Resistance (TEER)

The compounds' impact on the TEER of a differentiated monolayer grown in TW plates was assessed after 24 h and 48 h incubation time. Interestingly, after 24 h, all binary combinations of AOH, DON and UroA as well as AOH and DON alone led to a significant increase in TEER values (Figure 12A). Measurement of the second time point (48 h), however, revealed that 2.5 µM DON eventually decreased the TEER of the monolayer while the TEER of its binary combinations with UroA and AOH declined again to solvent control level (Figure 12B). After 48 h, treatment with AOH as well as UroA resulted in a significant increase in TEER. This effect was even exceeded when a binary combination of the two compounds was applied.

Inhibiting the AhR by adding the antagonistic CH223191 had no significant effect on the monolayer's response to neither UroA nor AOH regarding measured TEER values.

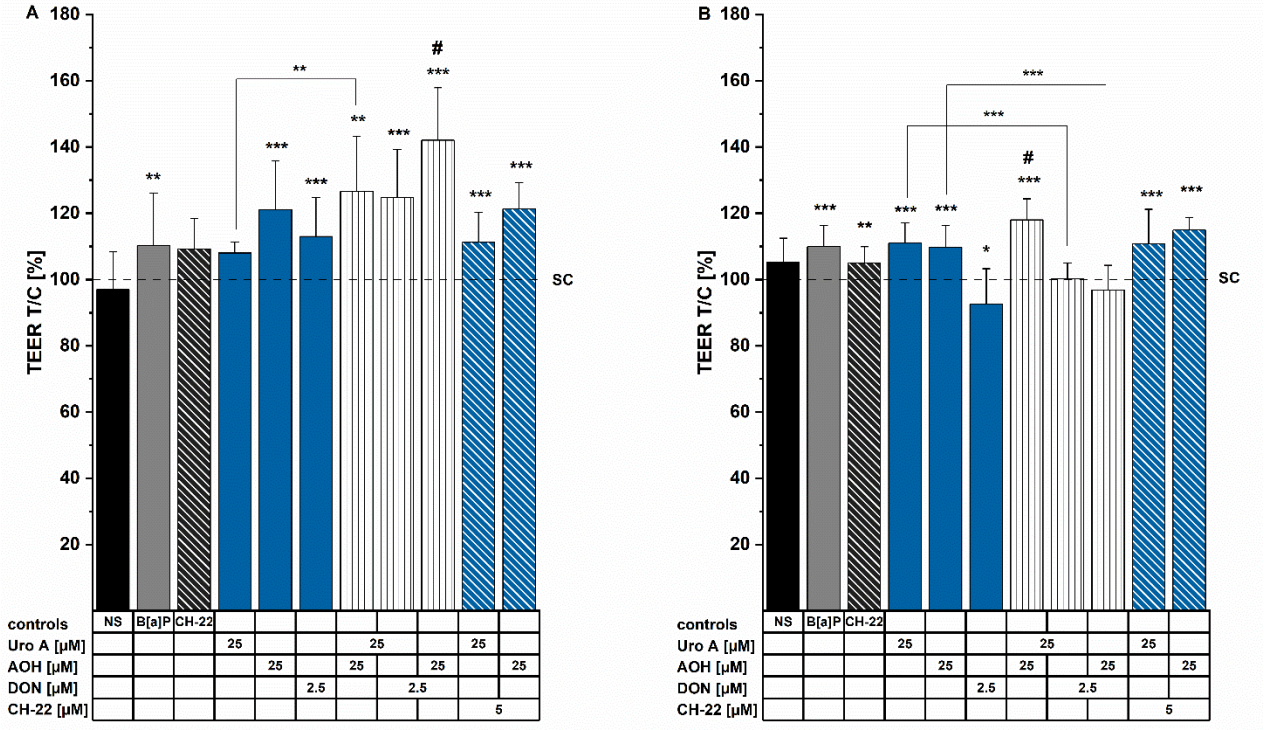

*Figure 12: TEER measurements of a differentiated Caco-2 monolayer conducted after A) 24 h and B) 48 h upon substance treatment, taken from Groestlinger et al. (2022a). $TEER_{REPORTED}$ [Ω*cm²] was normalised against the solvent control and plotted as percentage (T/C). Applied concentrations not stated in the figure are: B[a]P (5 µM) and CH-22 (5 µM); NS = no solvent. A two-sample Students' t-test was applied to calculate significant differences compared to the solvent control or between selected conditions which are shown as * (p<0.05), ** (p<0.01) and *** (p<0.001). # marks the significant difference of a binary incubation condition to both its constituents as single compounds with (p<0.05) at least.*

3.3.4 Permeability to Lucifer Yellow

In general, the three testing compounds did not exert drastic impacts on the monolayer's integrity regarding the passage of the LY dye. However, all binary combinations caused a slight yet significant increase in permeability compared to the solvent control (Figure 13). Amongst the single compound conditions, only AOH significantly enhanced permeability to LY. Notably, treatment with AOH simultaneously led to an increased TEER (Figure 12). In alignment with the TEER measurements, co-incubation of AOH with CH223191 did not counteract the effect of AOH.

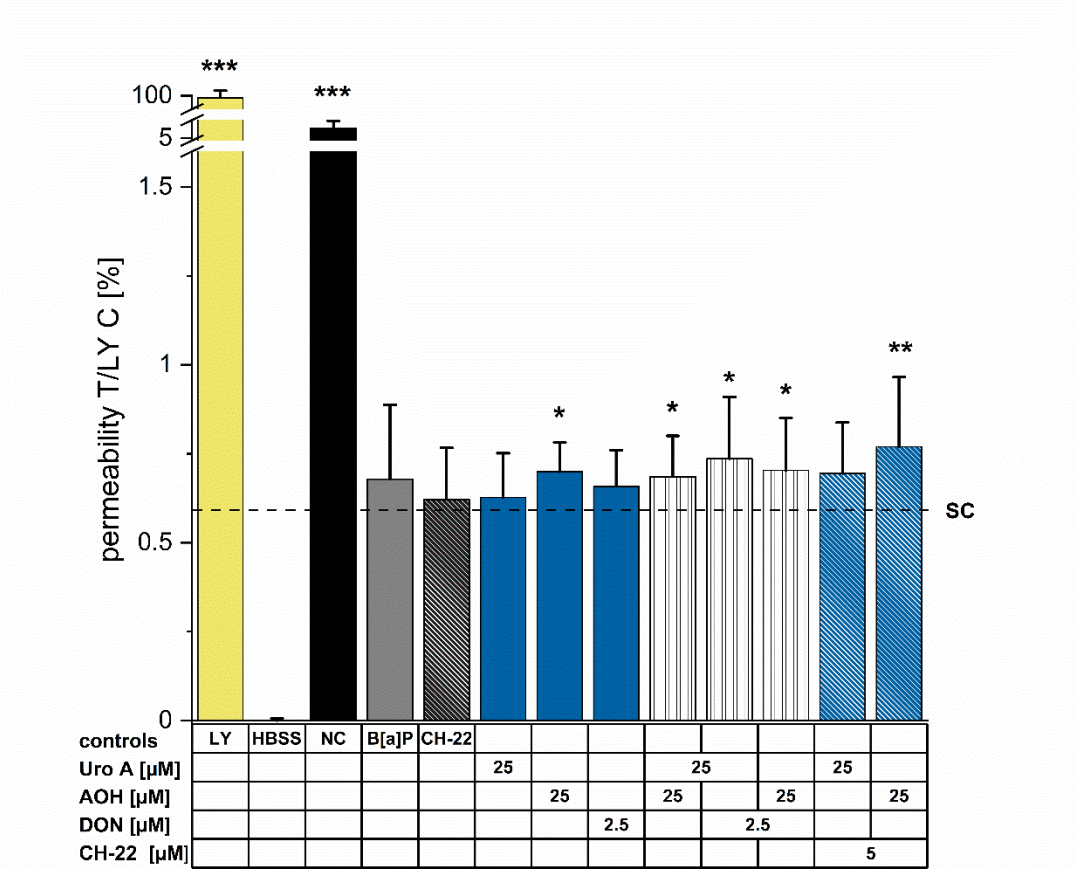

*Figure 13: Permeability assay assisted by Lucifer Yellow (LY) dye of a differentiated Caco-2 monolayer after treatment for 48 h, taken from Groestlinger et al. (2022a). Concentrations not stated in the figure are B[a]P (5 µM) and CH-22 (5 µM). HBSS buffer was measured alongside as control; NC (no cells) displays permeability of an empty insert. Pure dye (LY) was stipulated to a permeability of 100 %. The yield of the incubated conditions was normalised to pure LY, plotted as permeability [%] and compared to the solvent control (SC). A two-sample Students' t-test was applied to calculate significant differences compared to the solvent control or between selected conditions which are shown as * ($p<0.05$), ** ($p<0.01$) and *** ($p<0.001$).*

4 Discussion

This study investigated the impact of the two mycotoxins AOH and DON along with UroA, a gut microbial metabolite of ellagitannins, on the human intestinal epithelial barrier in an *in vitro* cell model. Additional focus was laid on the possible role of the AhR in the context of epithelial integrity and was determined by means of the AhR antagonist CH223191 and the reporter enzyme CYP1A1. AOH and UroA as well as the AhR agonist B[a]P, used as positive control, present planar molecules, as stated for the majority of AhR ligands defined so far (Schreck et al. 2012; Singh et al. 2019; Arenas-Huertero et al. 2019). Still, agonistic as well as antagonistic ligands are found in various categories and origins (Lamas et al. 2018). However, one should keep in mind that not every compound with the ability to regulate the AhR is also a direct ligand (Stockinger et al. 2021). Further, the downstream events upon AhR binding often appear tissue- and species-dependent. Safe et al. (2020) reviewed the multifaceted nature of AhR activation and propose AhR ligands to be so called "selective AhR modulators" for their AhR regulated effects show said specificity.

In the present study, AhR-dependent induction of EROD enzyme activity by AOH was found to be hindered in the presence of DON due to its inhibitory effect on protein translation. Both mycotoxins, DON and AOH led to reduced protein immunofluorescence signalling of CYP1A1 and the TJP ZO-1 (Figure 9, Figure 10). Intriguingly though, when applied as binary combination, signalling levels observed were similar to the solvent control level (CYP1A1) or even above (ZO-1). Further, examinations whether UroA has an impact on the toxins' effects within the colonic environment found that the addition of UroA alleviated the reduction of epithelial protein expression caused by the toxins *in vitro*.

Effect of the Mycotoxins on Activity and Protein Expression of CYP Isoforms

The AhR is not only capable of interfering with inflammatory pathways, it reportedly also plays a role in intestinal epithelial barrier function. Yu et al. (2018) found that AhR activation ameliorated inflammation status as well as impaired barrier function *in vitro* (Caco-2 cells) and *in vivo* (mice). Its activation prevented a decline in TEER and "morphological disruption" in regard to TJs caused by pro-inflammatory stimulation. Concurrent with the *in vitro* experiments, Yu et al. (2018) also described an alleviation in

the reduction of TJP expression (ZO-1, Cldn1, Occl) in the colonic mucosa of DSS-challenged mice. Since the intestinal barrier is particularly important when it comes to the defence against consumed food contaminants, compounds capable of interfering with such crucial regulatory systems urge thorough investigations. AOH has previously identified to induce the AhR/ARNT pathway and thereof dependent CYP1A1 expression (Schreck et al. 2012; Pahlke et al. 2016; Hohenbichler et al. 2020). The study at hand underpins the hypothesis, that AOH induces the enzyme activity of CYP1A1 in an AhR-dependent manner as no induction was observed in the presence of a known AhR-antagonist (Figure 7). Strikingly, IF staining revealed a marked decrease in CYP1A1 protein expression after AOH treatment (Figure 9). Although seemingly opposing, this effect was also regulated by the AhR since inhibition of the receptor did not lead to a decline but a slight increase in CYP1A1 expression. Of note, the EROD assay measures the enzyme activity of three different isoforms, namely CYP 1A1, 1A2 and 1B1, and not solely CYP1A1 (Donato 1993; Iwata et al. 2015). This could of course be a possible influencing factor but has not yet been investigated further. Another reasoning might be that cellular enzyme activity was boosted as compensational response to the decreased protein expression. In this case however, there would even occur a slight overcompensation as expression surpasses the basal level (Figure 9). DON alone did not exert prominent effects on EROD enzyme activity, but reduced CYP1A1 protein expression (Figure 9). The impact of DON on this AhR-regulated reporter enzyme is probably attributable to its mechanism of action of inhibiting protein synthesis and not to direct interactions with the AhR.

Impact on Tight Junction Proteins

As already mentioned, TJPs establish and regulate the intestinal barrier's integrity and permeability to a great part. Thus, studies repeatedly reported a loss of barrier function concomitantly with a reduced occurrence of different TJPs. The data presented show that both mycotoxins, AOH and DON, caused a reduction of the TJP ZO-1 in a differentiated Caco-2 monolayer (Figure 10). This matches the observed declining effect of DON on the TEER. The monolayers impaired resistance to ion passage might hence be ascribed to the depletion in TJP(s). Additional PCR analysis could further elucidate if the reduction is also apparent on translational level. Results from other studies with identical experimental parameters could not be found to compare this works' data to. There are, of course,

studies also investigating the abundance and localisation of TJPs after DON treatment, mostly with an exposure time of 24 h. In differentiated Caco-2 cells, neither Beisl et al. (2021) nor Luo et al. (2019) detected significant effects on the protein expression of ZO-1 at 1 and 10 µM or at 3, 10 and 30 µM DON, after 24 hours, respectively. While Wang et al. (2019) could not describe any effect on ZO-1 in "intermediately differentiated" (11 days) Caco-2 cells at 5 µM, cells that had differentiated for 21 days showed a receding trend in the abundance of ZO-1. Besides ZO-1, examples from other TJP groups like Occl and Cldn are also frequently examined in questions of epithelial barrier integrity. Luo et al. (2019) observed an apparent downward trend in the expression of Cldn4 and a decline of Occl in DON-challenged Caco-2 cells. A diminishing effect on Occl expression was also found by Wang et al. (2019). Intriguingly, they detected a decreased expression of Cldn4 in cells that differentiated for 21 days, while cells that were only given 11 days to differentiate revealed an increase of Cldn4. These results agree with Beisl et al. (2021) who observed an increased Cldn4 expression in Caco-2 cells that were treated with DON after seven days of differentiation as well as with van de Walle et al. (2010) who, again, revealed a reduction of Cldn4 in cells after 21 days of differentiation. Moreover, reduced expression of Cldn4, together with an unchanged Occl expression, was accompanied by an increase of the proteins' mRNA levels at a concentration of 5000 ng/ml DON. These observations highlight the fact, that the duration of the compound exposure, as well as status of the colonic barrier modulate the toxins' effect towards barrier proteins and epithelium integrity. In the case of AOH, the IF staining results did not align with the inclined TEER caused by AOH. The detected reduction of ZO-1 could, however, indicate a correlation with the enhanced permeability to LY upon AOH exposure. The cause of this discrepancy is yet to be explored. The consequence of AOH exposure on epithelial permeability is rarely investigated directly. There are however indirect ways through which it could have an impact on intestinal barrier integrity. As previously mentioned, AOH does have immunomodulatory potential (Schmutz et al. 2019; Solhaug et al. 2016a). This further affects the cells response to inflammatory stimuli and, as will be discussed later on, occurring inflammation can negatively influence intestinal epithelial barrier function. Also, its capability to generate ROS and induce oxidative stress bares potential to negatively impact TJP structure via MAPK signalling (Pahlke et al. 2016; Springler et al. 2016). Nevertheless, MAPKs were found to influence intestinal barrier function in an

improving but also impairing way, as summarised by Springler et al. (2016). Detailed investigation is therefore required to identify the critical parameters that enable the manipulation of such mechanisms in a health promoting way.

Consequences of UroA Treatment and Binary Combinations

The importance to investigate compounds' effects and risks not only in isolated scenarios but also in "co-presence" with other contaminants has already gained awareness. In addition to investigating combinatory effects of the two mycotoxins, UroA was added to the set-up to test it for the potential to influence the outcome of toxin exposure. As UroA is a direct ligand of the AhR (Muku et al. 2018), consequent effects on the intestinal barrier mediated via the AhR/ARNT pathway appear plausible. Muku et al. (2018) further found that the observed anti-inflammatory properties of the microbial metabolite are (at least partly) exerted in an AhR-dependent manner.

This work demonstrated that the microbial metabolite UroA enhanced enzyme activity through AhR activation (Figure 7), while protein expression of CYP1A1 was not impacted by UroA treatment (Figure 9). Interestingly, neither its effects on protein expression, contrary to AOH, nor the enhancement of the TEER were affected by inhibition of the AhR (Figure 9 to Figure 11; Figure 12B). Overall, UroA behaved similar, albeit to a lesser extent, to AOH in most experiments. This outcome might appear obvious since both are dibenzo-α-pyrones and share similar structures together with some biological properties (Aichinger 2021a). Strikingly though, one of them is a mycotoxin and one is handled as a potential therapeutic supplement. This discrepancy has been comprehensively discussed by Aichinger (2021a). Recalling however, AOH treatment also significantly enhanced enzyme activity (Figure 7A) while reducing the protein expression of the enzyme CYP1A1 (Figure 9). Despite the consideration that the IF data only present one while the EROD assay includes three CYP isoforms, this discrepancy could imply distinct AhR downstream effects upon activation by different ligands as addressed before. Nonetheless, under the EROD assay parameters applied, the two compounds acted in the same direction. Despite their AhR-dependent enhancement of enzyme activity, when combined, the two substances did not seem to exert an additive effect as the resulting induction did not deviate significantly from the one caused by AOH alone (Figure 7). AOH generally

displayed greater impact on enzyme activity which might hint at a higher affinity to the receptor in comparison to UroA.

Looking further at CYP1A1 protein expression, an interesting distinction is observable. While UroA appears to drive the outcome of binary treatments on protein expression, the effect of DON prevails when it comes to enzyme activity. More precisely, the presence of UroA prevented the decline of CYP1A1 expression, caused by both mycotoxins individually, yielding basal level (Figure 9). On the other hand, enzyme activity upon combinatory treatments involving DON revealed that DON hindered the increase caused by AOH and UroA individually, as can be seen in Figure 6. The substitution of DON for its human metabolite DON-3-Sulf, which does not interfere with protein synthesis (Warth et al. 2016), "preserved" the elevated enzyme activity levels in the binary combinations. This comparison confirms that DON's capability to inhibit protein synthesis plays a major role in the reduction it caused regarding the enzyme activity of CYP1A1, CYP1A2 and CYP1B1.

Remarkably, on the protein level the combination of AOH and DON exceeded the diminishing effects of both compounds individually, and even presented synergistic, by "remaining" at the same level as the solvent control. This was observable for CYP1A1 as well as ZO-1 protein expression, presented in Figure 9 and Figure 10, respectively. What lies behind these findings still needs to be deciphered. Arising questions whether co-presence of both toxins caused reciprocal hindering leaving "pre-existing" protein unaltered or if AOH "takes the place" of the structurally similar UroA in the presence of the potent toxin DON, also leading to basal levels of protein expression, are yet to be further investigated. For UroA and AOH, their effects on protein expression went in different directions, although they behaved similarly regarding EROD and TEER outcomes. This might be grounded on the differing modes of action. AOH induces single as well as double strand DNA breaks and is therefore able to cause impairment at transcriptional level (Fehr et al. 2009). The generation of ROS is reportedly one of the responsible mechanisms and was also observed in HT-29 as well as Caco-2 colon carcinoma cells (Fernández-Blanco et al. 2014; Pahlke et al. 2016). While DON interferes at protein translation level, no genotoxic mechanisms are known for UroA (Heilman et al. 2017). On the contrary, UroA is suggested to counteract oxidative stress (Aichinger 2021a; Luca et al. 2020).

Certain results, not only of this study, suggest a positive influence of compounds with a dibenzo-α-pyrone structure on the integrity of the intestinal barrier. The binary combination of AOH and UroA even exceeded the individual effects on TEER and TJP protein expression, suggesting potential for synergistic interaction (Figure 12B, Figure 10). As a remark, distinct definition of the combinatory interactions could not be performed with the data obtained. Other polyphenolic compounds have also been found to alleviate damage caused by mycotoxins. Delphinidin, for example, was able to suppress oxidative stress in HT-29 cells induced by AOH in a study by Aichinger et al. (2017). It also exerted antagonistic behaviour, as did genistein, against genotoxic effects of AOH in the comet assay. A study by Wang et al. (2019), referred to earlier, revealed that the product-derived antioxidant kaempferol in part mitigated or even prevented the detrimental effects of DON on the integrity of a Caco-2 monolayer in terms of TEER and TJP expression. In these regards, it would be interesting to assess if UroA also has the potential to attenuate genotoxic damage caused by AOH in ensuing experiments. Further research on combinatory interactions of mycotoxins and possibly alleviating nutritional compounds for deeper understanding and applications thus seems certainly worthwhile.

Integrity of the Intestinal Cells' Monolayer

The investigation of the mycotoxins' effects on direct parameters of intestinal barrier integrity revealed an increased TEER upon exposure to 2.5 µM DON for 24 h (Figure 12A). This reflects the results of Beisl et al. (2021) who also observed an increased TEER after 24 h of DON exposure in the same cell line, but no effect on the permeability to the flux marker LY. After 48 h, a decline of the TEER to around 90 % could be observed (Figure 12B), whereas permeability to LY was not impacted significantly (Figure 13). The factors causing this altered effect over time have so far not been further determined. It is imaginable that DON metabolites were formed and contributed to the effect on TEER. While conjugated derivates like DON-3-Sulf, for example, do not share the capability to inhibit protein translation, their effects on TEER and flux of the intestinal barrier could still be explored more closely. Further, enduring exposure to DON has an impact on the inflammatory state (van de Walle et al. 2008). This does not only impair via regulatory cytokines and activation of pathways like the MAPKs, but it also makes the cells more susceptible to protein loss as was found in the BCA assays (Figure 8). Contradictory to the

observations of Beisl et al. (2021) and those of this study, van de Walle et al. (2010) found a strong decrease of TEER in differentiated Caco-2 cells after exposure to 500 and 5000 ng/ml DON for 24 h as well as an increased permeability to the flux marker 2H-mannitol at 5000 ng/ml DON. These toxin concentrations correspond to about 1,7 and 17 µM (see Equation 2 in the supplementary data). The specific clone that was used is not stated, but it is of note that the cells were differentiated for a longer time period (21 days) before DON treatment. The findings of van de Walle et al. (2010) match those of Wang et al. (2019) who reported a decreased TEER as well as an increased flux of FD-4 in Caco-2 cells upon 24 h of exposure to 5 µM DON. The total differentiation time, yielding said results, also amounted to 21 days. Interestingly, the monolayer's response after "intermediate differentiation" (11 days) as well as the one by Beisl et al. (2021) with seven days of differentiation showed an increase in TEER values. These observations implicate that the initial reaction to DON of a Caco-2 monolayer regarding its permeability depends not only on the time of exposure but also the degree or "status" of cell differentiation. AOH, on the other hand, led to an increase in TEER values at both time points (24 h and 48 h) as well as in the permeability to LY (Figure 12; Figure 13). These findings might hint that different paths of transport are affected by AOH, explaining the contradictory results among different determinants of intestinal permeability. Besides, no related studies (suitable for comparison) assessing a direct correlation between AOH exposure and alterations in the integrity of the intestinal epithelial barrier, such as TEER or permeability assays, could be found. Therefore, this work hopefully contributes to the understanding of this debated "emerging" mycotoxin in the context of prevailing questions of intestinal barrier function.

Influence of and on an Inflammatory State

The complex network of mediators involved in inflammation, of course, also impacts the intestinal barrier properties in various ways. As for instance, TNF-α was found to cause redistribution of ZO-1 resulting in decreased TEER as well as enhanced permeability to larger molecules while IL-13 also reduced TEER but had no effect on paracellular flux (Farré et al. 2020). It is evident that the interplay of inflammatory cytokines and such can be very nuanced. Signalling routes like MAPKs and the NF-κB pathway can contribute to exacerbate inflammation upon their activation, e. g. after DON-induced ribotoxic stress or

aforementioned oxidative stress (van de Walle et al. 2008). Existing gastrointestinal inflammation can also trigger a decline of goblet cells leading to impaired mucin production and consequently a more vulnerable intestinal barrier (Amoroso et al. 2020). Ivanov et al. (2010) also reported structurally defective epithelial junctions *in vivo* in mice models with inflammation but also in human tissue samples of diseased patients. Although no marked differences between unstimulated and inflammatorily stimulated conditions were observed with the experiments of this study, the cells did reveal higher susceptibility in some assays if treated with IL-1β beforehand. This is most prominent in the cytotoxicity data. While cells without stimulus showed slight impairment by DON, alone and with AOH (Figure 5A), this effect was more pronounced for all conditions comprising DON under inflammatory conditions (Figure 5B). Aligning these results with the total protein content in Figure 8B, it becomes evident that inflammation leads to enhanced vulnerability of Caco-2 cells to the mycotoxin DON, most particularly its protein synthesis inhibitory mechanism. In addition, IL-1β stimulation led to decreased enzyme activity in untreated Caco-2 cells compared to the unstimulated solvent control (Figure 6B) but had no further remarkable effect on the cells' response to the testing conditions (data not shown).

5 Prospects and Conclusion

Reviewing the data and knowledge gathered so far, it becomes clear that the effects of the same substances often appear ambiguous. Although in some cases the reasons seem apparent, there is often room left for speculation due to inconsistent experimental parameters. While this is of course pivotal to depict and include various scenarios, a follow-up study combining and summarising a range of different set-ups to form a "comparable reference core" could be of additional aid. Aiming at the research topic of this study, such a combining study could include several key TJPs like Occl, Cldn4 and ZO-1, their protein expression as well as mRNA transcription levels, uniform concentration ranges, different CRC cell lines and various but coherent times of incubation as well as differentiation. As for the data obtained in the current study, some supplementary experiments appear intriguing like a competitive binding assay to determine if AOH induces AhR activity as a direct ligand or indirect activator. Furthermore, quantitative real-time PCR (q-RT PCR) analyses could provide a link between enzyme activity and IF staining data. q-RT PCR evaluation after 6 h of incubation revealed a strong suppression of CYP1A1 mRNA transcription for AOH, UroA and the binary combination thereof (Groestlinger et al. 2022a). Still, additional PCR analyses after 48 h of substance treatment would be of interest in order to potentially gain insight in the divergent results of enzyme activity and IF staining observed in the study at hand.

Greater understanding on effects and mechanism of bioactive compounds is not only employed to alleviate possible detriment but can also be used to improve public health. Substance groups associated with positive health effects like polyphenols are often incorporated in our diet via their original food or in form of supplements (Farré et al. 2020; Luca et al. 2020). Since urolithins were reported to provide protection for the GIT, especially by strengthening epithelial barrier function, they might also be qualified for such applications (Kujawska and Jodynis-Liebert 2020; Singh et al. 2019). Although urolithins are formed endogenously by the human microbiome, there is data that nevertheless emphasizes the potential benefit of direct supplementation. For one, not everyone's gut microbiota generates the metabolites UroA and UroB depending on the respective metabotype (Tomás-Barberán et al. 2017). Moreover, an *in vivo* study in rats by Larrosa et al. (2010) revealed that normal formation of urolithins was hampered in an

inflammatory state. Therefore, supplementation with UroA directly could be a way to circumvent interferences of diverse physiological conditions.

The findings presented in this thesis illustrate the detrimental impact that widely distributed food contaminants can have on the integrity of the intestinal epithelium. Nevertheless, they also demonstrate the potential of certain food derived compounds to protect this important biological barrier. Hopefully, this work can hence contribute to reduce occurring risks and join the efforts of making our food more secure and wholesome.

Abbreviations

Ac-DON	Acetyl-deoxynivalenol
AhR	Aryl hydrocarbon receptor
AhRR	AhR repressor
AME	Alternariol monomethyl ether
AMPs	Antimicrobial peptides
AOH	Alternariol
ARfD	Acute reference dose
ARNT	AhR nuclear traslocator
ATX-I	Altertoxin I
B[a]P	Benzo[*a*]pyrene
BCA	Bicinchoninic acid
BSA	Bovine serum albumin
Blebb	Blebbistatin
bw	Bodyweight
CD	Crohn's disease
Cldn	Claudin
CONTAM Panel	EFSA Panel on Contaminants in the Food Chain
CRC	Colorectal cancer
CTB	Cell Titer Blue
CYP	Cytochrome P450
CytD	Cytochalasin D
D3S/DON-3-Sulf	Deoxynivalenol-3-sulfate
DAPI	4',6-diamidino-2-phenylindole
Dex	Dexamethason
DMEM	Dulbecco's Modified Eagle Medium
DMSO	Dimethyl sulfoxide
DON	Deoxynivalenol
DON-3-Sulf/D3S	Deoxynivalenol-3-sulfate
DOM-1	Deepoxydeoxynivalenol
DPBS	Dulbecco's Phosphate Buffered Saline
DSS	Dextran sodium sulfate
EA	Ellagic acid
EFSA	European Food Safety Authority
7-ER	7-ethoxyresorufin
EROD	7-ethoxy-resorufin-*O*-deethylase
ETs	Ellagitannins
FA	Formaldehyde
FCS	Foetal calf serum
GIT	Gastrointestinal tract
HBSS	Hank's Balanced Salt Solution
IBD	Intestinal bowel diseases
IECs	Intestinal epithelial cells

IFN-γ	Interferon-γ
IL-1β	Interleukin-1β
IR	Infrared
isoUroA	Isourolithin A
LY	Lucifer Yellow
Mβ-CD	Methyl-β-cyclodextrin
MAPKs	Mitogen-activated protein kinases
NF-κB	Nuclear factor- κB
NR	Neutral Red
Occl	Occludin
OH-AOH	Hydroxyalternariol
PAH	Polycyclic aromatic hydrocarbon
PBS	Phosphate-buffered saline
q-RT PCR	quantitative real-time polymerase chain reaction
ROI	Region of interest
ROS	Reactive oxygen species
RT	Room temperature
SCFAs	Short chain fatty acids
SRB	Sulforhodamine B
TC	Tissue culture
TCA	Trichloroacetic acid
TCDD	2,3,7,8-tetrachlorodibenzo-p-dioxin
TDI	Tolerable daily intake
TeA	Tenuazonic acid
TEER	Transepithelial electrical resistance
TJ	Tight junctions
TJP	Tight junction protein
TNBS	2,4,6-trinitrobenzenesulfonic acid
TNF-α	Tumor necrosis factor-α
TTC	Threshold of toxicological concern
TW	Transwell
UC	Ulcerative colitis
UroA	Urolithin A
UroB	Urolithin B
ZO-1	Zona occludens-1

Supplements

Conversion of DON concentration from ng/ml to µM:

$$n = \frac{m}{M} = \frac{0.0005\ g}{296.32\ gmol^{-1}} \approx 1.687 \cdot 10^{-6}\ mol$$

$$c = \frac{n}{V} = \frac{1.687 \cdot 10^{-6}\ mol}{1\ L} \approx 1.7\ \mu M$$

Equation 2

β	.....	mass concentration [g/L]; here: 500 ng/mL ≙ 0.0005 g/L
c	.....	molar concentration [mol/L, µM]
m	.....	mass [g]
M	.....	molar mass [g/mol]; *M* (DON): 296.32 g/mol
n	.....	amount of substance [mol]
V	.....	volume [L]

Supplementary Experiments

Establishment of TEER Measurements with Sarstedt Inserts

Due to difficulties in the delivery of the TW plates by Corning® (routinely used at the institute), the method for TEER measurement of a differentiated monolayer of Caco-2 cells had to be re-established in TC-inserts from Sarstedt.

Consecutive assessment of the TEER over 21 days revealed higher alterations in TEER in the beginning and towards the end of the 21 days. The former visualizing the development of a tight monolayer by “closing” intercellular spaces. As illustrated in Suppl. Figure 1, the TEER values seemed to stabilize after approximately one week incorporating the seventh day which was subsequently the time of substance application.

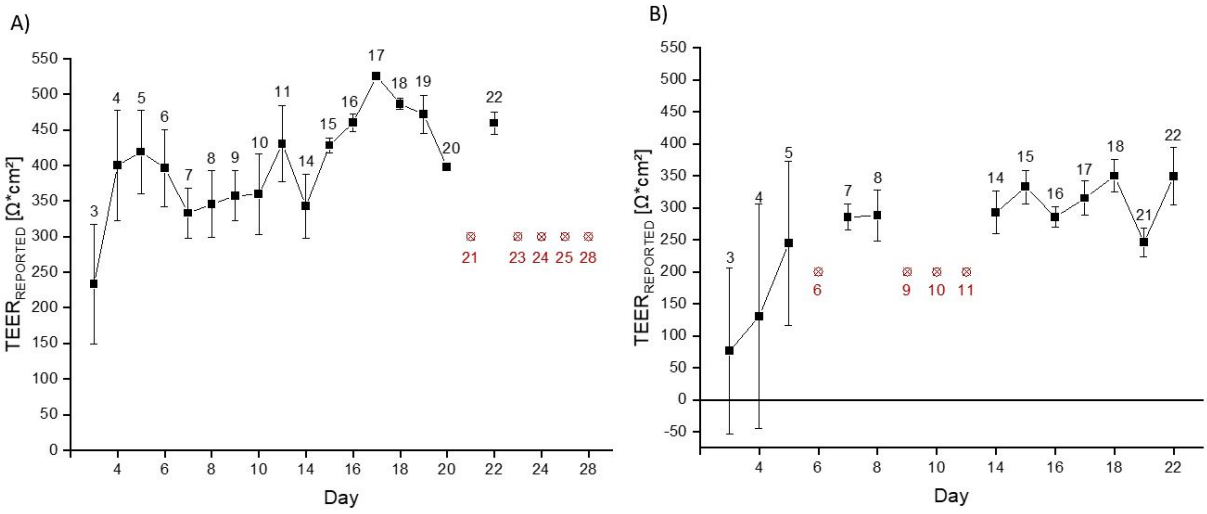

Suppl. Figure 1: TEER data of Caco-2 cell monolayers grown in A) Sarstedt "transparent" and B) Sarstedt "translucent" TC-inserts. Consecutive measurement of the TEER over at least 21 days. Data points marked with ⊗ represent cases in which it was not possible to obtain reliable data due to strong fluctuations of the voltohmeter.

Certain approaches and assays that were also performed within the framework of this study turned out not to be suitable for the cell model at use. Hence, they were not further pursued. Nonetheless, the methods applied are described in the following.

Cell Titer Blue (CTB) Cytotoxicity Assay

Cells were seeded in 96-well-plates at a density of 85.000 cells/cm² (24.650 cells per well). They were incubated for seven days under the conditions stated above before treatment with the substances of interest. One row was filled with PBS only (without any cells) to serve as blank. Medium was changed every two to three days. On the seventh day, culture medium was exchanged with incubation media and IL-1β was added to certain wells 2 h after application of the incubation solutions. After the desired exposure time (24 h), the incubation medium was removed and CTB solution (CTB concentrate diluted 1:10 in colourless DMEM) was added to each well before the plates were placed in the incubator at 37 °C for 45 min. CTB is a photosensitive dye, therefore it is necessary to work in the dark or with IR light during the entire assay. Viable cells are actively metabolizing the dye to a fluorescent product. Hence, 80 µl of the supernatant were transferred to a black 96-well-plate and fluorescence was measured at 590 nm_{em}/560 nm_{ex} using a plate reader (BioTek CytationTM 5 Multi Mode Reader).

Sulforhodamine B (SRB) Assay

Following the CTB assay, the Sulforhodamine B (SRB) assay was performed as an additional viability assay staining cellular proteins of living cells (Vichai and Kirtikara 2006). For this purpose, the supernatant remaining in the plate still containing the cells that were just subjected to the CTB assay was discarded. The plate was washed twice with ddH_2O and incubated with 50 µl 5 % trichloroacetic acid (TCA) per well for 1 h at 4 °C to fix the cells. Subsequently, the TCA solution was removed and three washing steps with ddH_2O were carried out. The plate was then dried overnight in the dark at RT. The following steps were performed in the dark or with IR light, since SRB is a photosensitive dye as well. Once the plate was completely dry, 50 µl SRB solution (4 % in 1 % acetic acid) were added to each well and incubated in the dark at RT for 1 h. After removing the former solution, the plate was washed twice with ddH_2O and once with 1 % acetic acid before being dried overnight again. To resolve the dye taken up by the cells, 100 µl of TRIS base were added and the plate was put on a shaker for 5 min. Finally, absorbance was measured at 570 nm using a plate reader (BioTek CytationTM 5 Multi Mode Reader).

Filipin Staining

Cell staining with the cholesterol-specific compound filipin is a method that allows the visualization of the cholesterol proportion in the cell membrane (Verstraeten et al. 2013). Preliminary experiments were performed to test if this could be an additional, applicable approach to gain information about the cell membranes of a Caco-2 monolayer and thus its integrity. For this purpose, cells were seeded in black cell culture plates with clear bottoms for immunofluorescence imaging and incubated under the conditions described earlier on. After 24 h of incubation time with the respective substances, the medium was discarded and the cells were washed with colourless DMEM. Subsequently, the cells were fixed with ≥ 1 % FA diluted in DPBS (see below), incubated for 15 min at RT and washed (colourless DMEM) afterwards. Then, a 100 mM glycine quenching solution (dissolved in DPBS) was applied to stop the FA reaction. Following another washing step with colourless DMEM, the filipin staining solution prepared in DPBS was added (see below for concentrations). In some cases, the cytoskeleton staining reagent phalloidin 488 was

included. After 1 h of incubation in the dark at RT, the cells were washed once more (colourless DMEM), covered with mounting medium (without DAPI) and imaged.

Both dyes, filipin and phalloidin, appeared too dense and saturated. Despite adaptations in the concentration of phalloidin 488 (diluted 1:500 and 1:1000), FA (1, 2, 3.7 and 5 %) and filipin (50, 10, 5 and 1 µg/ml), varying incubation times (0.5, 1 and 1.5 h) and duplicating the washing steps (including one on an orbital shaker), adequate microscopy images could not be obtained. Consequently, this approach was not further pursued.

Supplementary Data

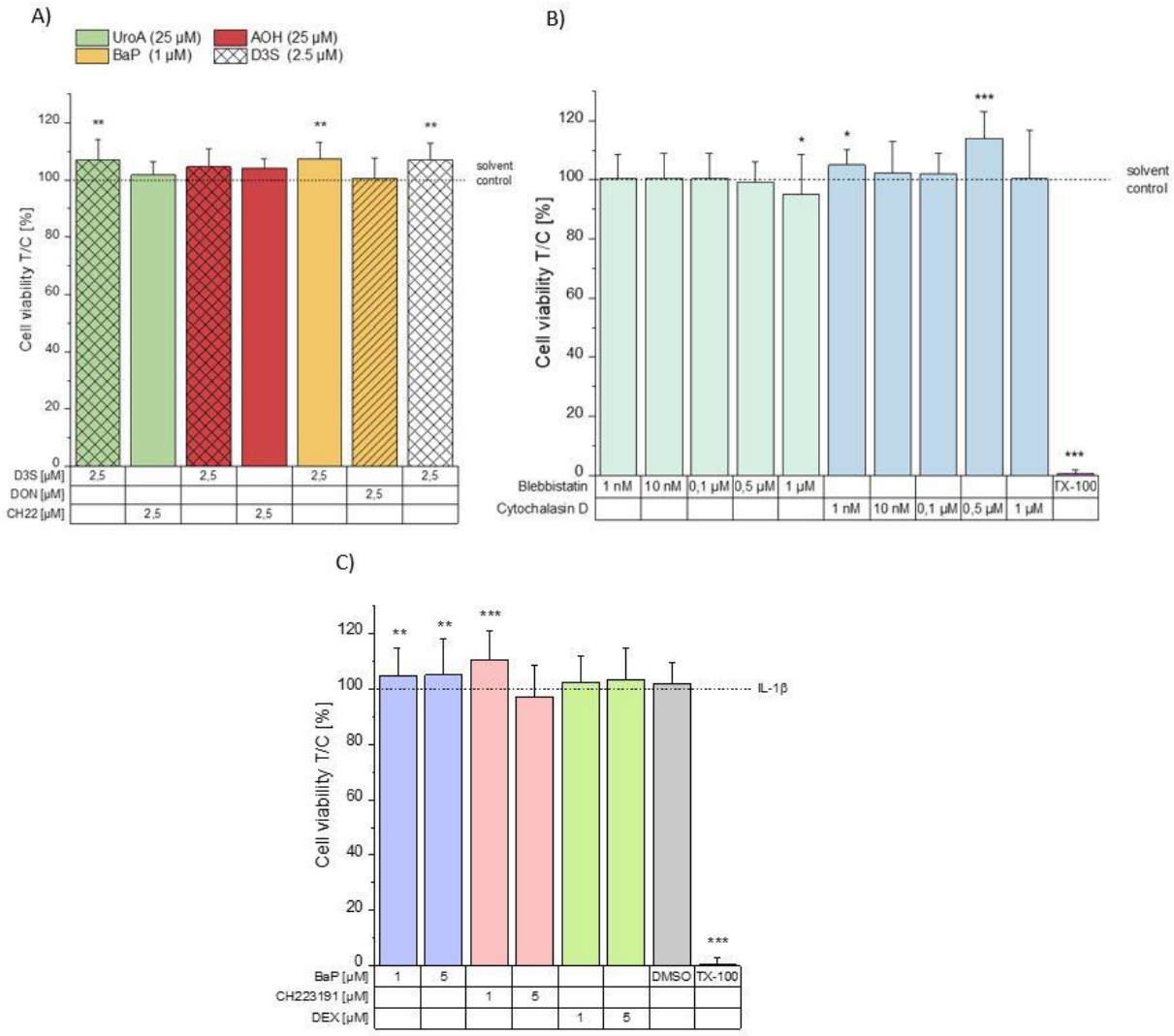

*Suppl. Figure 2: Neutral red data in Caco-2 cells A, B) after 48 h incubation time without IL-1ß stimulus and C) after 24 h incubation time with inflammatory IL-1ß stimulus. Results were normalised against the DMSO solvent control or IL-1ß solvent control and plotted as percentage (T/C). Two-sample Students' t-tests were applied to calculate significant differences compared to the respective solvent control which are shown as * (p<0.05), ** (p<0.01) and *** (p<0.001).*

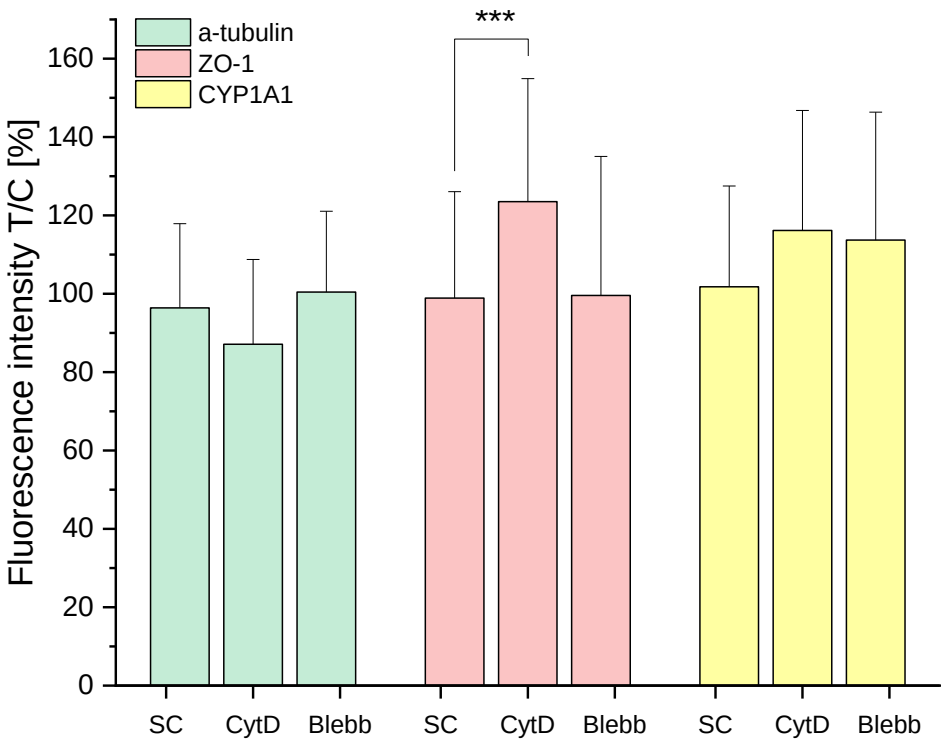

*Suppl. Figure 3: Fluorescence intensity representing protein expression of differentiated Caco-2 cells treated with blebbistatin (Blebb, 0.5 µM) and cytochalasin D (CytD, 0.5 µM) for 48 h. Values of the three different proteins were normalised to the respective solvent control (SC) and are depicted as T/C [%]. Significant differences were calculated applying a two-sample Students' t-test and are displayed as * (p<0.05), ** (p<0.01) and *** (p<0.001).*

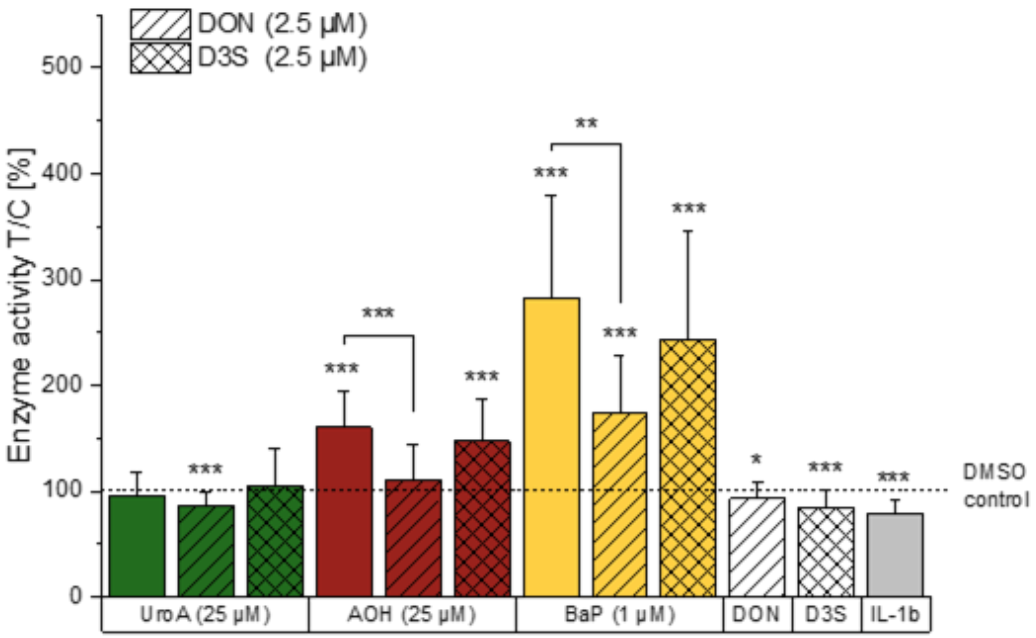

*Suppl. Figure 4: Enzyme activity (EROD assay) of Caco-2 cells after 48 h of substance incubation expressed as percentage (T/C). IL-1β stimulated treatments normalised against non-stimulated DMSO solvent control. Two-sample Students' t-tests were applied to calculate significant differences compared to the respective control which are shown as * (p<0.05), ** (p<0.01) and *** (p<0.001).*

Abstract (German)

Der Befall durch Schimmelpilze und die weitere Kontamination mit Mykotoxinen ist ein weltweites Problem, das pro Jahr etwa 25 % aller Nutzpflanzen betrifft. Derartige Kontaminanten bedeuten nicht nur einen möglichen Verlust von Rohstoffen, sondern stellen zum Teil auch ein gravierendes Gesundheitsrisiko für Mensch und Tier dar. Im Fokus der vorliegenden Arbeit stand der Einfluss der beiden prominenten Mykotoxine Deoxynivalenol (DON) und Alternariol (AOH) auf die Darmbarriere. Die Darmgesundheit und der dafür ausschlaggebende Entzündungsstatus hängen stark mit der Ernährung, aber auch dem Mikrobiom, zusammen. Daher wurde zusätzlich der Einfluss von Urolithin A (UroA), einem mikrobiellen Metaboliten der polyphenolischen Ellagitannine, auf die Darmbarriere untersucht. Es wurden unter anderem Enzymaktivitäten von CYP-Isoformen sowie Proteinexpression von CYP1A1 und dem Tight Junction Protein ZO-1 untersucht, da diese auf molekularer Ebene zur Barrierefunktion beitragen. Differenzierte Caco-2 Zellen bildeten das *in vitro*-Model eines humanen Darmepithels.

Die Experimente zeigten, dass UroA sowie AOH, mit einer Konzentration von 25 µM, die Enzymaktivität im EROD Assay nach 48 h signifikant erhöhen. In Kombination mit 2.5 µM DON blieben die Aktivitätslevel auf dem Niveau der Kontrolle. Gleichzeitig verringerte die Exposition gegenüber DON und AOH allein die Proteinexpression von CYP1A1 und von ZO-1. In Kombination miteinander, aber auch zusammen mit UroA, zeigten AOH und DON keinen Effekt auf die Expression von CYP1A1. Die Proteinexpression von ZO-1 hingegen übertraf das Level der Kontrolle sowie das von mindestens einer der Einzelsubstanzen in allen drei Szenarien binärer Kombination (AOH + DON, AOH + UroA, DON + UroA). Des Weiteren konnte bewiesen werden, dass sowohl UroA als auch AOH Regulatoren des Aryl-Hydrocarbon-Rezeptors (AhR) sind. Mithilfe des AhR-Antagonisten CH223191 wurde gezeigt, dass der Effekt von AOH und UroA auf die EROD-Enzymaktivität AhR-abhängig ist und im Fall von AOH auch der Effekt auf die untersuchte Proteinexpression.

Die Ergebnisse dieser Studie veranschaulichen, dass Lebensmittelkontaminanten wie Mykotoxine gezielt die Darmbarriere angreifen. Darüber hinaus konnten auch mögliche Ansätze aufgezeigt werden, dem entgegenzuwirken, beispielsweise durch gezielte Regulierung involvierter Signalwege oder die Einnahme bioaktiver Substanzen, die sich in die natürliche, menschliche Ernährung einbauen lassen.

List of Figures

References

Aichinger, Georg (2021a): Natural Dibenzo-α-Pyrones: Friends or Foes? In *International journal of molecular sciences* 22 (23). DOI: 10.3390/ijms222313063.

Aichinger, Georg; Beisl, Julia; Marko, Doris (2017): Genistein and delphinidin antagonize the genotoxic effects of the mycotoxin alternariol in human colon carcinoma cells. In *Molecular nutrition & food research* 61 (2). DOI: 10.1002/mnfr.201600462.

Aichinger, Georg; Del Favero, Giorgia; Warth, Benedikt; Marko, Doris (2021b): Alternaria toxins-Still emerging? In *Comprehensive reviews in food science and food safety* 20 (5), pp. 4390–4406. DOI: 10.1111/1541-4337.12803.

Amoroso, Chiara; Perillo, Federica; Strati, Francesco; Fantini, Massimo C.; Caprioli, Flavio; Facciotti, Federica (2020): The Role of Gut Microbiota Biomodulators on Mucosal Immunity and Intestinal Inflammation. In *Cells* 9 (5). DOI: 10.3390/cells9051234.

Arenas-Huertero, Francisco; Zaragoza-Ojeda, Montserrat; Sánchez-Alarcón, Juana; Milić, Mirta; Šegvić Klarić, Maja; Montiel-González, José M.; Valencia-Quintana, Rafael (2019): Involvement of Ahr Pathway in Toxicity of Aflatoxins and Other Mycotoxins. In *Frontiers in microbiology* 10, p. 2347. DOI: 10.3389/fmicb.2019.02347.

Beisl, Julia; Varga, Elisabeth; Braun, Dominik; Warth, Benedikt; Ehling-Schulz, Monika; Del Favero, Giorgia; Marko, Doris (2021): Assessing Mixture Effects of Cereulide and Deoxynivalenol on Intestinal Barrier Integrity and Uptake in Differentiated Human Caco-2 Cells. In *Toxins* 13 (3). DOI: 10.3390/toxins13030189.

Chen, Anqi; Mao, Xin; Sun, Qinghui; Wei, Zixuan; Li, Juan; You, Yanli et al. (2021): Alternaria Mycotoxins: An Overview of Toxicity, Metabolism, and Analysis in Food. In *Journal of agricultural and food chemistry* 69 (28), pp. 7817–7830. DOI: 10.1021/acs.jafc.1c03007.

Chou, Ting-Chao (2006): Theoretical basis, experimental design, and computerized simulation of synergism and antagonism in drug combination studies. In *Pharmacological reviews* 58 (3), pp. 621–681. DOI: 10.1124/pr.58.3.10.

Clarke, Gerard; Sandhu, Kiran V.; Griffin, Brendan T.; Dinan, Timothy G.; Cryan, John F.; Hyland, Niall P. (2019): Gut Reactions: Breaking Down Xenobiotic-Microbiome Interactions. In *Pharmacological reviews* 71 (2), pp. 198–224. DOI: 10.1124/pr.118.015768.

Cortés-Martín, A.; García-Villalba, R.; González-Sarrías, A.; Romo-Vaquero, M.; Loria-Kohen, V.; Ramírez-de-Molina, A. et al. (2018): The gut microbiota urolithin metabotypes revisited: the human metabolism of ellagic acid is mainly determined by aging. In *Food & function* 9 (8), pp. 4100–4106. DOI: 10.1039/c8fo00956b.

Crudo, Francesco; Varga, Elisabeth; Aichinger, Georg; Galaverna, Gianni; Marko, Doris; Dall'Asta, Chiara; Dellafiora, Luca (2019): Co-Occurrence and Combinatory Effects of Alternaria Mycotoxins and other Xenobiotics of Food Origin: Current Scenario and Future Perspectives. In *Toxins* 11 (11). DOI: 10.3390/toxins11110640.

Del Favero, Giorgia; Woelflingseder, Lydia; Braun, Dominik; Puntscher, Hannes; Kütt, Mary-Liis; Dellafiora, Luca et al. (2018): Response of intestinal HT-29 cells to the trichothecene mycotoxin deoxynivalenol and its sulfated conjugates. In *Toxicology letters* 295, pp. 424–437. DOI: 10.1016/j.toxlet.2018.07.007.

Dellafiora, Luca; Warth, Benedikt; Schmidt, Verena; Del Favero, Giorgia; Mikula, Hannes; Fröhlich, Johannes; Marko, Doris (2018): An integrated in silico/in vitro approach to assess the xenoestrogenic potential of Alternaria mycotoxins and metabolites. In *Food chemistry* 248, pp. 253–261. DOI: 10.1016/j.foodchem.2017.12.013.

Donato (1993): A Microassay for Measuring Cytochrome P450IA1 and P450IIB1 Activities in Intact Human and Rat Hepatocytes Cultured on 96-Well Plates. In *Analytical Biochemistry* (213), pp. 29–33.

EFSA (2011): Scientific Opinion on the risks for animal and public health related to the presence of Alternaria toxins in feed and food. In *EFSA Journal* 9 (10), p. 2407. DOI: 10.2903/j.efsa.2011.2407.

EFSA (2016): Dietary exposure assessment to Alternaria toxins in the European population. In *EFS2* 14 (12). DOI: 10.2903/j.efsa.2016.4654.

EFSA (2017): Scientific Opinion on the risks to human and animal health related to the presence of deoxynivalenol and its acetylated and modified forms in food and feed. In *EFSA journal. European Food Safety Authority* 15 (9), e04718. DOI: 10.2903/j.efsa.2017.4718.

EFSA (2022): Commission Recommendation (EU) 2022/553 on monitoring the presence of *Alternaria* toxins in food. In *Office Journal of the European Union*.

Escrivá, Laura; Oueslati, Souheib; Font, Guillermina; Manyes, Lara (2017): Alternaria Mycotoxins in Food and Feed: An Overview. In *Journal of Food Quality* 2017, pp. 1–20. DOI: 10.1155/2017/1569748.

Espín, Juan Carlos; Larrosa, Mar; García-Conesa, María Teresa; Tomás-Barberán, Francisco (2013): Biological significance of urolithins, the gut microbial ellagic Acid-derived metabolites: the evidence so far. In *Evidence-based complementary and alternative medicine : eCAM* 2013, p. 270418. DOI: 10.1155/2013/270418.

Fan, Kai; Guo, Wenbo; Huang, Qingwen; Meng, Jiajia; Yao, Qi; Nie, Dongxia et al. (2021): Assessment of Human Exposure to Five Alternaria Mycotoxins in China by Biomonitoring Approach. In *Toxins* 13 (11). DOI: 10.3390/toxins13110762.

Farré, Ricard; Fiorani, Marcello; Abdu Rahiman, Saeed; Matteoli, Gianluca (2020): Intestinal Permeability, Inflammation and the Role of Nutrients. In *Nutrients* 12 (4). DOI: 10.3390/nu12041185.

Fehr, Markus; Pahlke, Gudrun; Fritz, Jessica; Christensen, Morten O.; Boege, Fritz; Altemöller, Martina et al. (2009): Alternariol acts as a topoisomerase poison, preferentially affecting the IIalpha isoform. In *Molecular nutrition & food research* 53 (4), pp. 441–451. DOI: 10.1002/mnfr.200700379.

Fernández-Blanco, Celia; Font, Guillermina; Ruiz, Maria-Jose (2014): Oxidative stress of alternariol in Caco-2 cells. In *Toxicology letters* 229 (3), pp. 458–464. DOI: 10.1016/j.toxlet.2014.07.024.

Fernández-Blanco, Celia; Font, Guillermina; Ruiz, Maria-Jose (2015): Oxidative DNA damage and disturbance of antioxidant capacity by alternariol in Caco-2 cells. In *Toxicology letters* 235 (2), pp. 61–66. DOI: 10.1016/j.toxlet.2015.03.013.

Fernández-Blanco, Celia; Font, Guillermina; Ruiz, Maria-Jose (2016): Interaction effects of enniatin B, deoxinivalenol and alternariol in Caco-2 cells. In *Toxicology letters* 241, pp. 38–48. DOI: 10.1016/j.toxlet.2015.11.005.

Fraeyman, Sophie; Croubels, Siska; Devreese, Mathias; Antonissen, Gunther (2017): Emerging Fusarium and Alternaria Mycotoxins: Occurrence, Toxicity and Toxicokinetics. In *Toxins* 9 (7). DOI: 10.3390/toxins9070228.

Furlanetto, Valentina; Zagotto, Giuseppe; Pasquale, Riccardo; Moro, Stefano; Gatto, Barbara (2012): Ellagic acid and polyhydroxylated urolithins are potent catalytic inhibitors of human topoisomerase II: an in vitro study. In *Journal of agricultural and food chemistry* 60 (36), pp. 9162–9170. DOI: 10.1021/jf302600q.

Gao, Yanan; Meng, Lu; Liu, Huimin; Wang, Jiaqi; Zheng, Nan (2020): The Compromised Intestinal Barrier Induced by Mycotoxins. In *Toxins* 12 (10). DOI: 10.3390/toxins12100619.

Gaya, Pilar; Peirotén, Ángela; Medina, Margarita; Álvarez, Inmaculada; Landete, José M. (2018): Bifidobacterium pseudocatenulatum INIA P815: The first bacterium able to produce urolithins A and B from ellagic acid. In *Journal of Functional Foods* 45, pp. 95–99. DOI: 10.1016/j.jff.2018.03.040.

González-Sarrías, Antonio; Azorín-Ortuño, María; Yáñez-Gascón, María-Josefa; Tomás-Barberán, Francisco A.; García-Conesa, María-Teresa; Espín, Juan-Carlos (2009a): Dissimilar in vitro and in vivo effects of ellagic acid and its microbiota-derived metabolites, urolithins, on the cytochrome P450 1A1. In *Journal of agricultural and food chemistry* 57 (12), pp. 5623–5632. DOI: 10.1021/jf900725e.

González-Sarrías, Antonio; Espín, Juan-Carlos; Tomás-Barberán, Francisco A.; García-Conesa, María-Teresa (2009b): Gene expression, cell cycle arrest and MAPK signalling regulation in Caco-2 cells exposed to ellagic acid and its metabolites, urolithins. In *Molecular nutrition & food research* 53 (6), pp. 686–698. DOI: 10.1002/mnfr.200800150.

González-Sarrías, Antonio; Giménez-Bastida, Juan A.; García-Conesa, María T.; Gómez-Sánchez, María B.; García-Talavera, Noelia V.; Gil-Izquierdo, Angel et al. (2010a): Occurrence of urolithins, gut microbiota ellagic acid metabolites and proliferation markers expression response in the human prostate gland upon consumption of walnuts and pomegranate juice. In *Molecular nutrition & food research* 54 (3), pp. 311–322. DOI: 10.1002/mnfr.200900152.

González-Sarrías, Antonio; Giménez-Bastida, Juan Antonio; Núñez-Sánchez, María Ángeles; Larrosa, Mar; García-Conesa, María Teresa; Tomás-Barberán, Francisco A.; Espín, Juan Carlos (2014): Phase-II metabolism limits the antiproliferative activity of urolithins in human colon cancer cells. In *European journal of nutrition* 53 (3), pp. 853–864. DOI: 10.1007/s00394-013-0589-4.

González-Sarrías, Antonio; Larrosa, Mar; Tomás-Barberán, Francisco Abraham; Dolara, Piero; Espín, Juan Carlos (2010b): NF-kappaB-dependent anti-inflammatory activity of urolithins, gut microbiota ellagic acid-derived metabolites, in human colonic fibroblasts. In *The British journal of nutrition* 104 (4), pp. 503–512. DOI: 10.1017/S0007114510000826.

Grenier, Bertrand; Applegate, Todd J. (2013): Modulation of intestinal functions following mycotoxin ingestion: meta-analysis of published experiments in animals. In *Toxins* 5 (2), pp. 396–430. DOI: 10.3390/toxins5020396.

Groestlinger, Julia; Seidl, Carina; Varga, Elisabeth; Del Favero, Giorgia; Marko, Doris (2022a): Combinatory Exposure to Urolithin A, Alternariol, and Deoxynivalenol Affects Colon Cancer Metabolism and Epithelial Barrier Integrity in vitro. In *Frontiers in nutrition* 9, p. 882222. DOI: 10.3389/fnut.2022.882222.

Groestlinger, Julia; Spindler, Veronika; Pahlke, Gudrun; Rychlik, Michael; Del Favero, Giorgia; Marko, Doris (2022b): Alternaria alternata Mycotoxins Activate the Aryl Hydrocarbon Receptor and Nrf2-ARE Pathway to Alter the Structure and Immune Response of Colon Epithelial Cells. In *Chemical research in toxicology* 35 (5), pp. 731–749. DOI: 10.1021/acs.chemrestox.1c00364.

Gruber-Dorninger, Christiane; Novak, Barbara; Nagl, Veronika; Berthiller, Franz (2017): Emerging Mycotoxins: Beyond Traditionally Determined Food Contaminants. In *Journal of agricultural and food chemistry* 65 (33), pp. 7052–7070. DOI: 10.1021/acs.jafc.6b03413.

Heilman, Jacqueline; Andreux, Pénélope; Tran, Nga; Rinsch, Chris; Blanco-Bose, William (2017): Safety assessment of Urolithin A, a metabolite produced by the human gut microbiota upon dietary intake of plant derived ellagitannins and ellagic acid. In *Food and chemical toxicology : an international journal published for the British Industrial Biological Research Association* 108 (Pt A), pp. 289–297. DOI: 10.1016/j.fct.2017.07.050.

Hidalgo, Ismael J.; Raub, Thomas J.; Borchardt, Ronald T. (1989): Charachterization of the human colon carcinoma cell line (Caco-2) as a model system for intestinal epithelial permeability.

Ho, Wei-Ting; Chang, Jung-Shen; Chou, San-Fang; Hwang, Wei-Lun; Shih, Po-Jen; Chang, Shu-Wen et al. (2019): Targeting non-muscle myosin II promotes corneal endothelial migration through regulating lamellipodial dynamics. In *Journal of molecular medicine (Berlin, Germany)* 97 (9), pp. 1345–1357. DOI: 10.1007/s00109-019-01818-5.

Hohenbichler, Julia; Aichinger, Georg; Rychlik, Michael; Del Favero, Giorgia; Marko, Doris (2020): Alternaria alternata Toxins Synergistically Activate the Aryl Hydrocarbon Receptor Pathway In Vitro. In *Biomolecules* 10 (7). DOI: 10.3390/biom10071018.

Ivanov, Andrei I.; Parkos, Charles A.; Nusrat, Asma (2010): Cytoskeletal regulation of epithelial barrier function during inflammation. In *The American journal of pathology* 177 (2), pp. 512–524. DOI: 10.2353/ajpath.2010.100168.

Iwata, Hisato; Yamaguchi, Keisuke; Takeshita, Yoko; Kubota, Akira; Hirakawa, Shusaku; Isobe, Tomohiko et al. (2015): Enzymatic characterization of in vitro-expressed Baikal seal cytochrome P450 (CYP) 1A1, 1A2, and 1B1: implication of low metabolic potential of CYP1A2 uniquely evolved in aquatic mammals. In *Aquatic toxicology (Amsterdam, Netherlands)* 162, pp. 138–151. DOI: 10.1016/j.aquatox.2015.03.010.

Jalimarada, Supriya S.; Shivanna, Mahesh; Kini, Vidisha; Mehta, Dolly; Srinivas, Sangly P. (2009): Microtubule disassembly breaks down the barrier integrity of corneal endothelium. In *Experimental eye research* 89 (3), pp. 333–343. DOI: 10.1016/j.exer.2009.03.019.

Kasimsetty, Sashi G.; Bialonska, Dobroslawa; Reddy, Muntha K.; Ma, Guoyi; Khan, Shabana I.; Ferreira, Daneel (2010): Colon cancer chemopreventive activities of pomegranate ellagitannins and urolithins. In *Journal of agricultural and food chemistry* 58 (4), pp. 2180–2187. DOI: 10.1021/jf903762h.

Koppel, Nitzan; Maini Rekdal, Vayu; Balskus, Emily P. (2017): Chemical transformation of xenobiotics by the human gut microbiota. In *Science (New York, N.Y.)* 356 (6344). DOI: 10.1126/science.aag2770.

Krautkramer, Kimberly A.; Fan, Jing; Bäckhed, Fredrik (2021): Gut microbial metabolites as multi-kingdom intermediates. In *Nature reviews. Microbiology* 19 (2), pp. 77–94. DOI: 10.1038/s41579-020-0438-4.

Kujawska, Małgorzata; Jodynis-Liebert, Jadwiga (2020): Potential of the ellagic acid-derived gut microbiota metabolite - Urolithin A in gastrointestinal protection. In *World journal of gastroenterology* 26 (23), pp. 3170–3181. DOI: 10.3748/wjg.v26.i23.3170.

Lamas, Bruno; Natividad, Jane M.; Sokol, Harry (2018): Aryl hydrocarbon receptor and intestinal immunity. In *Mucosal immunology* 11 (4), pp. 1024–1038. DOI: 10.1038/s41385-018-0019-2.

Larrosa, Mar; González-Sarrías, Antonio; Yáñez-Gascón, María J.; Selma, María V.; Azorín-Ortuño, María; Toti, Simona et al. (2010): Anti-inflammatory properties of a pomegranate extract and its metabolite urolithin-A in a colitis rat model and the effect of colon inflammation on phenolic metabolism. In *The Journal of nutritional biochemistry* 21 (8), pp. 717–725. DOI: 10.1016/j.jnutbio.2009.04.012.

Le Shen; Weber, Christopher R.; Raleigh, David R.; Yu, Dan; Turner, Jerrold R. (2011): Tight junction pore and leak pathways: a dynamic duo. In *Annual review of physiology* 73, pp. 283–309. DOI: 10.1146/annurev-physiol-012110-142150.

Lee, Hyang Burm; Patriarca, Andrea; Magan, Naresh (2015a): Alternaria in Food: Ecophysiology, Mycotoxin Production and Toxicology. In *Mycobiology* 43 (2), pp. 93–106. DOI: 10.5941/MYCO.2015.43.2.93.

Lee, Sung Hee (2015b): Intestinal permeability regulation by tight junction: implication on inflammatory bowel diseases. In *Intestinal research* 13 (1), pp. 11–18. DOI: 10.5217/ir.2015.13.1.11.

Luca, Simon Vlad; Macovei, Irina; Bujor, Alexandra; Miron, Anca; Skalicka-Woźniak, Krystyna; Aprotosoaie, Ana Clara; Trifan, Adriana (2020): Bioactivity of dietary polyphenols: The role of metabolites. In *Critical reviews in food science and nutrition* 60 (4), pp. 626–659. DOI: 10.1080/10408398.2018.1546669.

Luo, Su; Terciolo, Chloe; Bracarense, Ana Paula F. L.; Payros, Delphine; Pinton, Philippe; Oswald, Isabelle P. (2019): In vitro and in vivo effects of a mycotoxin, deoxynivalenol, and a trace metal, cadmium, alone or in a mixture on the intestinal barrier. In *Environment international* 132, p. 105082. DOI: 10.1016/j.envint.2019.105082.

Mayorgas, Aida; Dotti, Isabella; Salas, Azucena (2021): Microbial Metabolites, Postbiotics, and Intestinal Epithelial Function. In *Molecular nutrition & food research* 65 (5), e2000188. DOI: 10.1002/mnfr.202000188.

McLaughlin, John; Padfield, Philip J.; Burt, Julian P. H.; O'Neill, Catherine A. (2004): Ochratoxin A increases permeability through tight junctions by removal of specific claudin isoforms. In *American journal of physiology. Cell physiology* 287 (5), C1412-7. DOI: 10.1152/ajpcell.00007.2004.

Mishra, Sakshi; Srivastava, Sonal; Dewangan, Jayant; Divakar, Aman; Kumar Rath, Srikanta (2020): Global occurrence of deoxynivalenol in food commodities and exposure risk assessment in humans in the last decade: a survey. In *Critical reviews in food science and nutrition* 60 (8), pp. 1346–1374. DOI: 10.1080/10408398.2019.1571479.

Muku, Gulsum E.; Murray, Iain A.; Espín, Juan C.; Perdew, Gary H. (2018): Urolithin A Is a Dietary Microbiota-Derived Human Aryl Hydrocarbon Receptor Antagonist. In *Metabolites* 8 (4). DOI: 10.3390/metabo8040086.

Nuñez-Sánchez, María A.; García-Villalba, Rocío; Monedero-Saiz, Tamara; García-Talavera, Noelia V.; Gómez-Sánchez, María B.; Sánchez-Álvarez, Carmen et al. (2014): Targeted metabolic

profiling of pomegranate polyphenols and urolithins in plasma, urine and colon tissues from colorectal cancer patients. In *Molecular nutrition & food research* 58 (6), pp. 1199–1211. DOI: 10.1002/mnfr.201300931.

Odenwald, Matthew A.; Turner, Jerrold R. (2017): The intestinal epithelial barrier: a therapeutic target? In *Nature reviews. Gastroenterology & hepatology* 14 (1), pp. 9–21. DOI: 10.1038/nrgastro.2016.169.

Pahlke, G.; Tiessen, C.; Domnanich, K.; Kahle, N.; Groh, I. A. M.; Schreck, I. et al. (2016): Impact of Alternaria toxins on CYP1A1 expression in different human tumor cells and relevance for genotoxicity. In *Toxicology letters* 240 (1), pp. 93–104. DOI: 10.1016/j.toxlet.2015.10.003.

Pfeiffer, Erika; Schebb, Nils H.; Podlech, Joachim; Metzler, Manfred (2007): Novel oxidative in vitro metabolites of the mycotoxins alternariol and alternariol methyl ether. In *Molecular nutrition & food research* 51 (3), pp. 307–316. DOI: 10.1002/mnfr.200600237.

Pinton, Philippe; Braicu, Cornelia; Nougayrede, Jean-Philippe; Laffitte, Joëlle; Taranu, Ionelia; Oswald, Isabelle P. (2010): Deoxynivalenol impairs porcine intestinal barrier function and decreases the protein expression of claudin-4 through a mitogen-activated protein kinase-dependent mechanism. In *The Journal of nutrition* 140 (11), pp. 1956–1962. DOI: 10.3945/jn.110.123919.

Pinton, Philippe; Tsybulskyy, Dima; Lucioli, Joelma; Laffitte, Joëlle; Callu, Patrick; Lyazhri, Faouzi et al. (2012): Toxicity of deoxynivalenol and its acetylated derivatives on the intestine: differential effects on morphology, barrier function, tight junction proteins, and mitogen-activated protein kinases. In *Toxicological sciences : an official journal of the Society of Toxicology* 130 (1), pp. 180–190. DOI: 10.1093/toxsci/kfs239.

Ponce de León-Rodríguez, Maria Del Carmen; Guyot, Jean-Pierre; Laurent-Babot, Caroline (2019): Intestinal in vitro cell culture models and their potential to study the effect of food components on intestinal inflammation. In *Critical reviews in food science and nutrition* 59 (22), pp. 3648–3666. DOI: 10.1080/10408398.2018.1506734.

Repetto, Guillermo; del Peso, Ana; Zurita, Jorge L. (2008): Neutral red uptake assay for the estimation of cell viability/cytotoxicity.

Safe, Stephen; Jin, Un-Ho; Park, Hyejin; Chapkin, Robert S.; Jayaraman, Arul (2020): Aryl Hydrocarbon Receptor (AHR) Ligands as Selective AHR Modulators (SAhRMs). In *International journal of molecular sciences* 21 (18). DOI: 10.3390/ijms21186654.

Schiwy, Andreas; Brinkmann, Markus; Thiem, Ines; Guder, Gabriele; Winkens, Kerstin; Eichbaum, Kathrin et al. (2015): Determination of the CYP1A-inducing potential of single substances, mixtures and extracts of samples in the micro-EROD assay with H4IIE cells. In *Nature protocols* 10 (11), pp. 1728–1741. DOI: 10.1038/nprot.2015.108.

Schmutz, Cornelia; Cenk, Ebru; Marko, Doris (2019): The Alternaria Mycotoxin Alternariol Triggers the Immune Response of IL-1β-stimulated, Differentiated Caco-2 Cells. In *Molecular nutrition & food research* 63 (20), e1900341. DOI: 10.1002/mnfr.201900341.

Schoultz, Ida; Keita, Åsa V. (2019): Cellular and Molecular Therapeutic Targets in Inflammatory Bowel Disease-Focusing on Intestinal Barrier Function. In *Cells* 8 (2). DOI: 10.3390/cells8020193.

Schreck, Ilona; Deigendesch, Ute; Burkhardt, Britta; Marko, Doris; Weiss, Carsten (2012): The Alternaria mycotoxins alternariol and alternariol methyl ether induce cytochrome P450 1A1 and

apoptosis in murine hepatoma cells dependent on the aryl hydrocarbon receptor. In *Archives of toxicology* 86 (4), pp. 625–632. DOI: 10.1007/s00204-011-0781-3.

Schreiber, S.; Nikolaus, S.; Hampe, J. (1998): Activation of nuclear factor kappa B inflammatory bowel disease. In *Gut* 42 (4), pp. 477–484. DOI: 10.1136/gut.42.4.477.

Selma, María V.; Beltrán, David; García-Villalba, Rocío; Espín, Juan C.; Tomás-Barberán, Francisco A. (2014): Description of urolithin production capacity from ellagic acid of two human intestinal Gordonibacter species. In *Food & function* 5 (8), pp. 1779–1784. DOI: 10.1039/c4fo00092g.

Singh, Rajbir; Chandrashekharappa, Sandeep; Bodduluri, Sobha R.; Baby, Becca V.; Hegde, Bindu; Kotla, Niranjan G. et al. (2019): Enhancement of the gut barrier integrity by a microbial metabolite through the Nrf2 pathway. In *Nature communications* 10 (1), p. 89. DOI: 10.1038/s41467-018-07859-7.

Solhaug, A.; Karlsøen, L. M.; Holme, J. A.; Kristoffersen, A. B.; Eriksen, G. S. (2016a): Immunomodulatory effects of individual and combined mycotoxins in the THP-1 cell line. In *Toxicology in vitro : an international journal published in association with BIBRA* 36, pp. 120–132. DOI: 10.1016/j.tiv.2016.07.012.

Solhaug, Anita; Eriksen, Gunnar S.; Holme, Jørn A. (2016b): Mechanisms of Action and Toxicity of the Mycotoxin Alternariol: A Review. In *Basic & clinical pharmacology & toxicology* 119 (6), pp. 533–539. DOI: 10.1111/bcpt.12635.

Springler, Alexandra; Hessenberger, Sabine; Schatzmayr, Gerd; Mayer, Elisabeth (2016): Early Activation of MAPK p44/42 Is Partially Involved in DON-Induced Disruption of the Intestinal Barrier Function and Tight Junction Network. In *Toxins* 8 (9). DOI: 10.3390/toxins8090264.

Stockinger, Brigitta; Shah, Kathleen; Wincent, Emma (2021): AHR in the intestinal microenvironment: safeguarding barrier function. In *Nature reviews. Gastroenterology & hepatology* 18 (8), pp. 559–570. DOI: 10.1038/s41575-021-00430-8.

Tiessen, Christine; Ellmer, Doris; Mikula, Hannes; Pahlke, Gudrun; Warth, Benedikt; Gehrke, Helge et al. (2017): Impact of phase I metabolism on uptake, oxidative stress and genotoxicity of the emerging mycotoxin alternariol and its monomethyl ether in esophageal cells. In *Archives of toxicology* 91 (3), pp. 1213–1226. DOI: 10.1007/s00204-016-1801-0.

Tomás-Barberán, Francisco A.; García-Villalba, Rocío; González-Sarrías, Antonio; Selma, María V.; Espín, Juan C. (2014): Ellagic acid metabolism by human gut microbiota: consistent observation of three urolithin phenotypes in intervention trials, independent of food source, age, and health status. In *Journal of agricultural and food chemistry* 62 (28), pp. 6535–6538. DOI: 10.1021/jf5024615.

Tomás-Barberán, Francisco A.; González-Sarrías, Antonio; García-Villalba, Rocío; Núñez-Sánchez, María A.; Selma, María V.; García-Conesa, María T.; Espín, Juan Carlos (2017): Urolithins, the rescue of "old" metabolites to understand a "new" concept: Metabotypes as a nexus among phenolic metabolism, microbiota dysbiosis, and host health status. In *Molecular nutrition & food research* 61 (1). DOI: 10.1002/mnfr.201500901.

van de Walle, Jacqueline; Romier, Béatrice; Larondelle, Yvan; Schneider, Yves-Jacques (2008): Influence of deoxynivalenol on NF-kappaB activation and IL-8 secretion in human intestinal Caco-2 cells. In *Toxicology letters* 177 (3), pp. 205–214. DOI: 10.1016/j.toxlet.2008.01.018.

van de Walle, Jacqueline; Sergent, Thérèse; Piront, Neil; Toussaint, Olivier; Schneider, Yves-Jacques; Larondelle, Yvan (2010): Deoxynivalenol affects in vitro intestinal epithelial cell barrier

integrity through inhibition of protein synthesis. In *Toxicology and applied pharmacology* 245 (3), pp. 291–298. DOI: 10.1016/j.taap.2010.03.012.

van der Fels-Klerx, H. J.; Liu, C.; Battilani, P. (2016): Modelling climate change impacts on mycotoxin contamination. In *World Mycotoxin Journal* 9 (5), pp. 717–726. DOI: 10.3920/WMJ2016.2066.

van Tran, Nguyen; Viktorová, Jitka; Ruml, Tomáš (2020): Mycotoxins: Biotransformation and Bioavailability Assessment Using Caco-2 Cell Monolayer. In *Toxins* 12 (10). DOI: 10.3390/toxins12100628.

Vejdovszky, Katharina; Warth, Benedikt; Sulyok, Michael; Marko, Doris (2016): Non-synergistic cytotoxic effects of Fusarium and Alternaria toxin combinations in Caco-2 cells. In *Toxicology letters* 241, pp. 1–8. DOI: 10.1016/j.toxlet.2015.10.024.

Verstraeten, Sandra V.; Jaggers, Grayson K.; Fraga, Cesar G.; Oteiza, Patricia I. (2013): Procyanidins can interact with Caco-2 cell membrane lipid rafts: involvement of cholesterol. In *Biochimica et biophysica acta* 1828 (11), pp. 2646–2653. DOI: 10.1016/j.bbamem.2013.07.023.

Vichai, Vanicha; Kirtikara, Kanyawim (2006): Sulforhodamine B colorimetric assay for cytotoxicity screening. In *Nature protocols* 1 (3), pp. 1112–1116. DOI: 10.1038/nprot.2006.179.

Wang, Xiaojie; Li, Li; Zhang, Genyi (2019): Impact of deoxynivalenol and kaempferol on expression of tight junction proteins at different stages of Caco-2 cell proliferation and differentiation. In *RSC Adv.* 9 (59), pp. 34607–34616. DOI: 10.1039/C9RA06222J.

Warth, Benedikt; Del Favero, Giorgia; Wiesenberger, Gerlinde; Puntscher, Hannes; Woelflingseder, Lydia; Fruhmann, Philipp et al. (2016): Identification of a novel human deoxynivalenol metabolite enhancing proliferation of intestinal and urinary bladder cells. In *Scientific reports* 6, p. 33854. DOI: 10.1038/srep33854.

Yu, Min; Wang, Qimeng; Ma, Yuanhang; Li, Liangzi; Yu, Kun; Zhang, Zhicao et al. (2018): Aryl Hydrocarbon Receptor Activation Modulates Intestinal Epithelial Barrier Function by Maintaining Tight Junction Integrity. In *International journal of biological sciences* 14 (1), pp. 69–77. DOI: 10.7150/ijbs.22259.

Zhao, Bin; Degroot, Danica E.; Hayashi, Ai; He, Guochun; Denison, Michael S. (2010): CH223191 is a ligand-selective antagonist of the Ah (Dioxin) receptor. In *Toxicological sciences : an official journal of the Society of Toxicology* 117 (2), pp. 393–403. DOI: 10.1093/toxsci/kfq217.